

# ColPali: EFFICIENT DOCUMENT RETRIEVAL WITH VISION LANGUAGE MODELS

**Anonymous authors**

Paper under double-blind review

## ABSTRACT

Documents are visually rich structures that convey information through text, but also figures, page layouts, tables, or even fonts. Since modern retrieval systems mainly rely on the textual information they extract from document pages to index documents -often through lengthy and brittle processes-, they struggle to exploit key visual cues efficiently. This limits their capabilities in many practical document retrieval applications such as Retrieval Augmented Generation (RAG). To benchmark current systems on visually rich document retrieval, we introduce the Visual Document Retrieval Benchmark *ViDoRe*, composed of various page-level retrieval tasks spanning multiple domains, languages, and practical settings. The inherent complexity and performance shortcomings of modern systems motivate a new concept; doing document retrieval by directly embedding the images of the document pages. We release *ColPali*, a Vision Language Model trained to produce high-quality multi-vector embeddings from images of document pages. Combined with a late interaction matching mechanism, *ColPali* largely outperforms modern document retrieval pipelines while being drastically simpler, faster and end-to-end trainable. We release models, data, code and benchmarks under open licenses at <https://hf.co/<anonymous>>.

## 1 INTRODUCTION

Document Retrieval consists of matching a user query to relevant documents in a given corpus. It is central to many widespread industrial applications, either as a standalone ranking system (search engines) or as part of more complex information extraction or Retrieval Augmented Generation (RAG) pipelines.

Over recent years, pretrained language models have enabled large improvements in text embedding models. In practical industrial settings, however, the primary performance bottleneck for efficient document retrieval stems not from embedding model performance but from the prior data ingestion pipeline. To index a standard PDF document, many steps are required. First, PDF parsers or Optical Character Recognition (OCR) systems are used to extract words from the pages. Document layout detection models can then be run to segment paragraphs, titles, and other page objects such as tables, figures, and headers. A chunking strategy is then defined to group text passages with some semantical coherence, and modern retrieval setups may even integrate a captioning step to describe visually rich elements in a natural language form, more suitable for embedding models. In our experiments (Table 2), we typically find that optimizing the ingestion pipeline yields much better performance on visually rich document retrieval than optimizing the text embedding model.

**Contribution 1: *ViDoRe*.** In this work, we argue that document retrieval systems should not be evaluated solely on the capabilities of text embedding models (Bajaj et al., 2016; Thakur et al., 2021; Muennighoff et al., 2022), but should also consider the context and visual elements of the documents to be retrieved. To this end, we create and openly release *ViDoRe*, a comprehensive benchmark to evaluate systems on page-level document retrieval with a wide coverage of domains, visual elements, and languages. *ViDoRe* addresses practical document retrieval scenarios, where queries often necessitate both textual and visual understanding for accurate document matching. We highlight the shortcomings of current text-centric systems in these settings.<sup>1</sup>

<sup>1</sup>The benchmark leaderboard is hosted publicly at <https://huggingface.co/spaces/<anonymous>> to encourage further developments.

054  
055  
056  
057  
058  
059  
060  
061  
062  
063  
064  
065  
066  
067  
068  
069  
070  
071  
072  
073  
074  
075  
076  
077  
078  
079  
080  
081  
082  
083  
084  
085  
086  
087  
088  
089  
090  
091  
092  
093  
094  
095  
096  
097  
098  
099  
100  
101  
102  
103  
104  
105  
106  
107

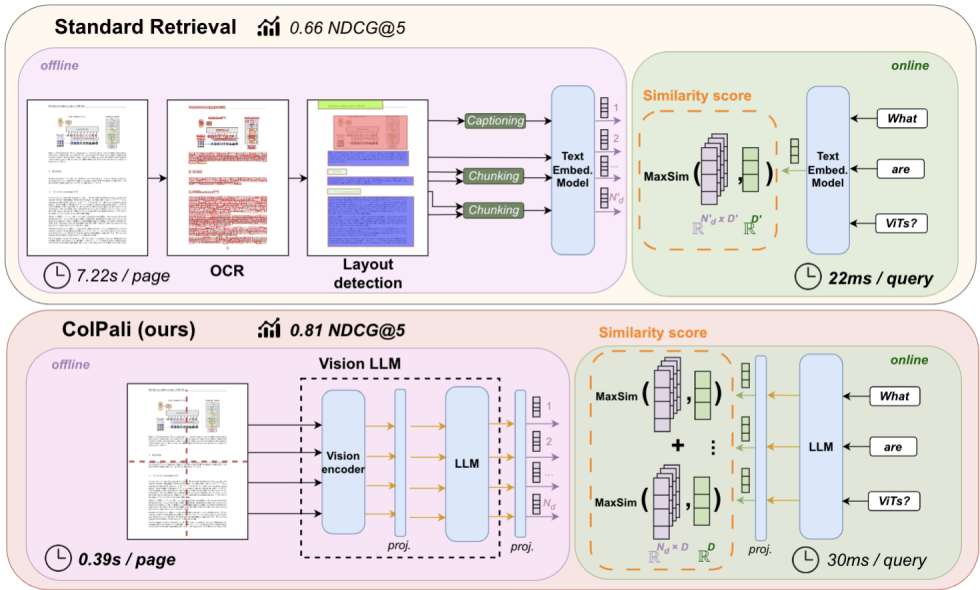


Figure 1: *ColPali* simplifies document retrieval w.r.t. standard retrieval methods while achieving stronger performances with better latencies. Latencies and results are detailed in section 5 and subsection B.4.

**Contribution 2: ColPali.** We propose a novel concept and model architecture based on Vision Language Models (VLMs) to efficiently index documents purely from their visual features, allowing for subsequent fast query matching with late interaction mechanisms (Khattab & Zaharia, 2020). Our method, *ColPali*, significantly outperforms all other retrieval systems on *ViDoRe* while being fast and end-to-end trainable. These results demonstrate the potential and the many benefits of this novel *Retrieval in Vision Space* concept, which could significantly alter the way document retrieval is approached in the industry moving forward. We release all resources at [https://hf.co/\(anonymous\)](https://hf.co/(anonymous)).

## 2 PROBLEM FORMULATION & RELATED WORK

**Problem Setting.** In our setting, a retrieval system scores how relevant a document  $d$  from corpus  $\mathcal{D}$  is with respect to a query  $q$ . Computing the similarity score  $s(q, d) \in \mathbb{R}$  for each of the  $|\mathcal{D}|$  documents in the corpus creates a ranking we can use to extract the most relevant documents. In this work, we focus on page-level retrieval: *given a query, is the correct document page retrieved by the system?* For coherence with existing literature, we further use the term *document* to refer to individual pages, i.e. the atomic retrieved elements in our setting. As we focus on practical industrial retrieval applications (RAG, search engines) with potentially large corpora sizes, latency constraints are imposed on scoring systems. Most current retrieval systems can be decomposed into (1) an *offline* indexation phase in which a document index is built and (2) an *online* querying phase in which a query is matched to documents from the index and where low latency is vital to the user experience.

*Under these industrial constraints, we identify three main properties an efficient document retrieval systems should exhibit: (R1) strong retrieval performance, as measured by standard retrieval metrics; (R2) fast online querying, measured through average latencies; (R3) high throughput corpus indexation, ie. the number of pages that can be embedded in a given timeframe.*

### 2.1 TEXTUAL RETRIEVAL METHODS

**Document Retrieval in Text Space.** Statistical methods based on word frequency like TF-IDF (Sparck Jones, 1972) and BM25 (Robertson et al., 1994) are still widely used due to their simplicity and efficiency. More recently, neural embedding models based on fine-tuned large language models

display state-of-the-art performance on a variety of text embedding tasks and top the retrieval leaderboards (Muennighoff et al., 2022).

**Neural Retrievers.** In bi-encoder models (Reimers & Gurevych, 2019; Karpukhin et al., 2020; Wang et al., 2022), documents are independently mapped *offline* to a dense vector space. Queries are embedded *online* and matched to documents through a fast cosine distance computation. A slower, but slightly more performant alternative, cross-encoder systems (Wang et al., 2020; Cohere, 2024) concatenate query and document as a single input sequence and iteratively attribute matching scores to each possible combination. This enables full attention computation between query and document terms but comes at the cost of computational efficiency, as  $|\mathcal{D}|$  encoding passes must be done online.

**Multi-Vector retrieval via late interaction.** In the late interaction paradigm introduced by ColBERT (Khattab & Zaharia, 2020), an embedding is pre-computed and indexed per document token. At runtime, similarity can be computed with individual query token embeddings. The idea is to benefit from the rich interaction between individual query and document terms while taking advantage of the offline computation and fast query matching enabled by bi-encoders. [See section E for more details.](#)

**Retrieval Evaluation.** Although benchmarks and leaderboards have been developed to evaluate text embedding models (Thakur et al., 2021; Muennighoff et al., 2022), much of the performance improvements in industrial use cases of embedding models stem from the prior data ingestion pipeline. While documents often rely on visual elements to more efficiently convey information to human readers, text-only systems barely tap into these visual cues. Other work has also independently studied table or chart retrieval systems through repurposed Question Answering datasets (Zhang et al., 2019; Nowak et al., 2024) but only assessing specialized methods for each task.

*To our knowledge, no benchmark evaluates document retrieval systems in practical settings; in an end-to-end manner; across several document types and topics, and by evaluating the use of both textual and visual document features.*

## 2.2 INTEGRATING VISUAL FEATURES

**Contrastive Vision Language Models.** Mapping latent representations of textual content to corresponding representations of visual content has been done by aligning disjoint visual and text encoders through contrastive losses (Radford et al., 2021; Zhai et al., 2023). While some OCR capabilities exist in these models, the visual component is often not optimized for text understanding. The Fine-grained Interactive Language-Image Pre-training (Yao et al., 2021) framework extends the late interaction mechanism to cross-modal vision-language models, relying on max similarity operations between text tokens and image patches.

**Visually Rich Document Understanding.** To go beyond text, some document-focused models jointly encode text tokens alongside visual or document layout features (Appalaraju et al., 2021; Kim et al., 2021; Huang et al., 2022; Tang et al., 2022). Large Language transformer Models (LLMs) with strong reasoning capabilities have recently been combined with Vision Transformers (ViTs) (Dosovitskiy et al., 2020) to create VLMs (Alayrac et al., 2022; Liu et al., 2023; Bai et al., 2023; Laurençon et al., 2024b) where image patch vectors from contrastively trained ViT models (Zhai et al., 2023) are fed as input embeddings to the LLM and concatenated with the text-token embeddings.

**PaliGemma.** The PaliGemma-3B model (Beyer et al., 2024) extends concepts from Pali3 (Chen et al., 2023), and projects SigLIP-So400m/14 (Alabdulmohsin et al., 2023) patch embeddings into Gemma-2B’s text vector space (Gemma Team et al., 2024). Along with its reasonable size w.r.t. other performant VLMs, an interesting property of PaliGemma’s text model is that it is fine-tuned with full-block attention on the prefix (instruction text and image tokens). [See Appendix E for more details.](#)

*VLMs display enhanced capabilities in Visual Question Answering, captioning, and document understanding (Yue et al., 2023), but are not optimized for retrieval tasks.*

## 3 THE ViDoRe BENCHMARK

Existing benchmarks for contrastive vision-language models primarily evaluate retrieval for natural images (Lin et al., 2014; Borchmann et al., 2021; Thapliyal et al., 2022). On the other hand, textual

retrieval benchmarks (Muennighoff et al., 2022) are evaluated at at textual passage level and are not tailored for document retrieval tasks. We fill the gap with *ViDoRe*, a comprehensive benchmark for document retrieval using visual features.

### 3.1 BENCHMARK DESIGN

*ViDoRe* is designed to comprehensively evaluate retrieval systems on their capacity to match queries to relevant documents at the page level. This benchmark encompasses multiple orthogonal subtasks, with focuses on various modalities - text, figures, infographics, tables; thematic domains - medical, business, scientific, administrative; or languages - English, French. Tasks also span varying levels of complexity, in order to capture signals from both weaker and stronger systems. As many systems require large amounts of time to index pages (captioning-based approaches can take dozens of seconds per page for instance), we limit the number of candidate documents for each retrieval task in order to evaluate even complex systems in a reasonable timeframe without sacrificing quality. For trainable retrieval systems, we provide a reference training set that can be used to facilitate comparisons.

Dataset	Language	# Queries	# Documents	Description
<b>Academic Tasks</b>				
DocVQA	English	500	500	Scanned documents from UCSF Industry
InfoVQA	English	500	500	Infographics scrapped from the web
TAT-DQA	English	1600	1600	High-quality financial reports
arXivQA	English	500	500	Scientific Figures from arXiv
TabFQuAD	French	210	210	Tables scrapped from the web
<b>Practical Tasks</b>				
Energy	English	100	1000	Documents about energy
Government	English	100	1000	Administrative documents
Healthcare	English	100	1000	Medical documents
AI	English	100	1000	Scientific documents related to AI
Shift Project	French	100	1000	Environmental reports

Table 1: *ViDoRe* comprehensively evaluates multimodal retrieval methods.

**Academic Tasks.** We repurpose widely used visual question-answering benchmarks for retrieval tasks: for each page-question-answer triplet, we use the question as the query, and the associated page as the gold document (Table 1). These academic datasets either focus on single specific modalities (Mathew et al., 2020; 2021; Li et al., 2024) or target more varied visually rich documents (Zhu et al., 2022). Moreover, we consider TabFQuAD, a human-labeled dataset on tables extracted from French industrial PDF documents released with this work. Details can be found in subsection A.1.

**Practical tasks.** We construct topic-specific retrieval benchmarks spanning multiple domains to go beyond repurposed QA datasets and evaluate retrieval in more realistic industrial situations (e.g. RAG). To achieve this, we collect publicly accessible PDF documents and generate queries pertaining to document pages using Claude-3 Sonnet, a high-quality proprietary vision-language model (Anthropic, 2024). In total, we collect 1,000 document pages per topic, which we associate with 100 queries extensively filtered for quality and relevance by human annotators. The corpus topics are intentionally specific to maximize syntactic proximity between documents, creating more challenging retrieval tasks and covering an array of orthogonal domains (Table 1).<sup>2</sup>

**Evaluation Metrics.** We evaluate performance on our benchmark (Requirement R1) using standard metrics from the retrieval literature (nDCG, Recall@K, MRR). We report nDCG@5 values as the main performance metric in this work and release the complete sets of results along with the models<sup>3</sup>. To validate compliance with practical industrial requirements (section 2), we also consider query latencies (R2) and indexing throughputs (R3).

<sup>2</sup>Answers are generated alongside queries to (1) ground queries and improve their quality and (2) provide resources to foster future work.

<sup>3</sup><https://hf.co/<anonymous>>

### 3.2 ASSESSING CURRENT SYSTEMS

**Unstructured.** We evaluate retrieval systems representative of those found in standard industrial RAG pipelines. As is common practice, we rely on the Unstructured<sup>4</sup> off-the-shelf tool in the highest resolution settings to construct high-quality text chunks from PDF documents. Unstructured orchestrates the document parsing pipeline, relying on deep learning vision models to detect titles and document layouts (Ge et al., 2021), OCR engines (Smith, 2007) to extract text in non-native PDFs, specialized methods or models to detect and reconstruct tables, and implements a chunking strategy (by-title) that leverages the detected document structure to preserve section boundaries when concatenating texts. As is common practice, in our simplest Unstructured configuration (*text-only*), only textual elements are kept and figures, images, and tables are considered noisy information and are filtered out.

**Unstructured + X.** While Unstructured is a strong baseline by itself, we further augment Unstructured’s output by integrating the visual elements. In (+ *OCR*), tables, charts, and images are run through an OCR engine, processed by Unstructured, and chunked independently. In (+ *Captioning*), we set up a fully-fledged captioning strategy (Zhao et al., 2023), in which we feed visual elements to a strong proprietary Vision Language Model (Claude-3 Sonnet (Anthropic, 2024)) to obtain highly detailed textual descriptions of the elements. Both strategies aim to integrate visual elements in the retrieval pipeline but incur significant latency and resource costs (subsection 5.2).

**Embedding Model.** To embed textual chunks, we evaluate Okapi BM25, the *de facto* standard sparse statistical retrieval method, and the dense encoder of BGE-M3 (Chen et al., 2024), a multilingual neural method with SOTA performance in its size category. Chunks are embedded and scored independently, and page-level scores are obtained by max-pooling over the page’s chunk scores.<sup>5</sup>

**Contrastive VLMs.** We also evaluate the strongest available vision-language embedding models; Jina CLIP (Koukounas et al., 2024), Nomic Embed Vision (Nomic, 2024), and SigLIP-So400m/14 (Alabdulmohsin et al., 2023).

**Results.** From a performance perspective, best results are obtained by combining the Unstructured parser with visual information, either from captioning strategies or by running OCR on the visual elements (Table 2). Little difference is seen between BM25 and BGE-M3 embeddings highlighting the visual information bottleneck. Contrastive VLMs lag behind. Beyond retrieval performance (R1), the indexing latencies (R2) reported in Figure 2 illustrate that PDF parsing pipelines can be very lengthy, especially when incorporating OCR or captioning strategies. Querying latencies at runtime (R3) are very good for all evaluated systems ( $\leq 22$  ms on a NVIDIA L4) due to fast query encoding and cosine similarity matching.

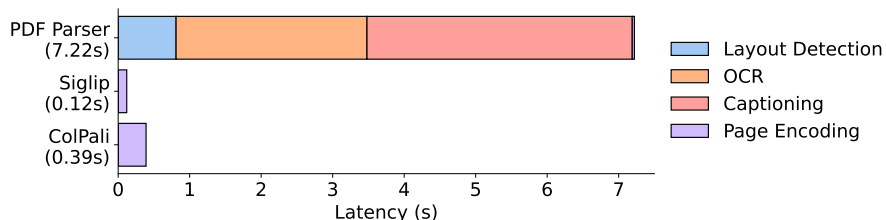


Figure 2: Offline document indexing with *ColPali* is much simpler and faster compared to standard retrieval methods. The PDF Parser results are obtained following the *Unstructured* settings with BGE-M3 detailed in subsection 3.2. All indexing speeds are averaged per-page latencies. More details in subsection B.4.

<sup>4</sup>[www.unstructured.io](http://www.unstructured.io)

<sup>5</sup>We empirically validated the max-pooling strategy over sub-page chunks to be more effective than concatenating all page chunks before embedding pagewise.

## 4 LATE INTERACTION BASED VISION RETRIEVAL

### 4.1 ARCHITECTURE

**Vision-Language Models.** Encouraged by their strong document understanding capabilities, we propose adapting recent VLMs for retrieval. The key concept is to leverage the alignment between output embeddings of text and image tokens acquired during multi-modal fine-tuning. To this extent, we introduce *ColPali*, a PaliGemma-3B extension that is capable of generating ColBERT-style multi-vector representations of text and images (Figure 1). PaliGemma-3B is a strong candidate due to its small size, the many released checkpoints fine-tuned for different image resolutions and tasks, and the promising performances on various document understanding benchmarks. We add a projection layer to map **each of the language model’s output token embeddings (whether from text or image tokens)** to a vector space of reduced dimension  $D = 128$  as used in the ColBERT paper (Khattab & Zaharia, 2020) to keep lightweight bag-of-embedding representations.

**Late Interaction.** Given query  $q$  and document  $d$ , we denote as  $\mathbf{E}_q \in \mathbb{R}^{N_q \times D}$  and  $\mathbf{E}_d \in \mathbb{R}^{N_d \times D}$  their respective multi-vector representation in the common embedding space  $\mathbb{R}^D$ , **where  $N_q$  and  $N_d$  are respectively the number of vectors in the query and in the document page embeddings**. The late interaction operator,  $\text{LI}(q, d)$ , is the sum over all query vectors  $\mathbf{E}_q^{(j)}$ , of its maximum dot product  $\langle \cdot | \cdot \rangle$  with each of the  $N_d$  document embedding vectors  $\mathbf{E}_d^{(1:N_d)}$ .

$$\text{LI}(q, d) = \sum_{i \in [1, N_q]} \max_{j \in [1, N_d]} \langle \mathbf{E}_q^{(i)} | \mathbf{E}_d^{(j)} \rangle \quad (1)$$

**Contrastive Loss.** The Late Interaction operation is fully differentiable, enabling backpropagation. Let a batch  $\{q_k, d_k\}_{k \in [1, b]}$  composed of  $b$  query-page pairs, where for all  $k \in [1, b]$ , the document page  $d_k$  is the document corresponding to query  $q_k$ . Following Khattab & Zaharia (2020), we define our in-batch contrastive loss  $\mathcal{L}$  as the softmaxed cross-entropy of the positive scores  $s_k^+ = \text{LI}(q_k, d_k)$  w.r.t. to the maximal in-batch negative scores  $s_k^- = \max_{l, l \neq k} \text{LI}(q_k, d_l)$ <sup>6</sup>:

$$\mathcal{L} = -\frac{1}{b} \sum_{k=1}^b \log \left[ \frac{\exp(s_k^+)}{\exp(s_k^+) + \exp(s_k^-)} \right] = \frac{1}{b} \sum_{k=1}^b \log(1 + \exp(s_k^- - s_k^+)) \quad (2)$$

### 4.2 MODEL TRAINING

**Dataset.** Our training dataset of 118,695 query-page pairs is comprised of train sets of openly available academic datasets (63%) and a synthetic dataset made up of pages from web-crawled PDF documents and augmented with VLM-generated (Claude-3 Sonnet) pseudo-questions (37%). Dataset split details are given in subsection A.3. Our training set is fully English by design, enabling us to study zero-shot generalization to non-English languages<sup>7</sup>. We explicitly verify no multi-page PDF document is used both *ViDoRe* and in the train set to prevent evaluation contamination. A validation set is created with 2% of the samples to tune hyperparameters. We openly release the training dataset<sup>8</sup> for reproducibility and to encourage further research.

**Parameters.** All models are trained for 1 epoch on the train set. Unless specified otherwise, we train models in bfloat16 format, use low-rank adapters (LoRA, Hu et al. (2021)) with  $\alpha = 32$  and  $r = 32$  on the transformer layers from the language model, as well as the final randomly initialized projection layer, and use a paged\_adamw\_8bit optimizer. We train on an 8 GPU setup with data parallelism, a learning rate of  $5e - 5$  with linear decay with 2.5% warmup steps, and a batch size of 32.

**Query Augmentation.** As in Khattab & Zaharia (2020), we append 5 <unused0> tokens to the query tokens to serve as a soft, differentiable query expansion or re-weighting mechanism.

<sup>6</sup>We reformulate the loss to leverage the numerically stable softplus function where  $\text{softplus}(x) = \log(1 + \exp(x))$

<sup>7</sup>Multilingual data is present in the pretraining corpus of the language model (Gemma-2B) and potentially occurs during PaliGemma-3B’s multimodal training.

<sup>8</sup>[https://huggingface.co/datasets/\(anonymous\)](https://huggingface.co/datasets/(anonymous))

## 5 RESULTS

	ArxivQ	DocQ	InfoQ	TabF	TATQ	Shift	AI	Energy	Gov.	Health.	Avg.
<b>Unstructured text-only</b>											
- BM25	-	34.1	-	-	44.0	59.6	90.4	78.3	78.8	82.6	-
- BGE-M3	-	28.4 <sub>↓5.7</sub>	-	-	36.1 <sub>↓7.9</sub>	68.5 <sub>↑8.9</sub>	88.4 <sub>↓2.0</sub>	76.8 <sub>↓1.5</sub>	77.7 <sub>↓1.1</sub>	84.6 <sub>↑2.0</sub>	-
<b>Unstructured + OCR</b>											
- BM25	31.6	36.8	62.9	46.5	62.7	64.3	92.8	85.9	83.9	87.2	65.5
- BGE-M3	31.4 <sub>↓0.2</sub>	25.7 <sub>↓11.1</sub>	60.1 <sub>↓2.8</sub>	70.8 <sub>↑24.3</sub>	50.5 <sub>↓12.2</sub>	<b>73.2</b> <sub>↑8.9</sub>	90.2 <sub>↓2.6</sub>	83.6 <sub>↓2.3</sub>	84.9 <sub>↑1.0</sub>	91.1 <sub>↑3.9</sub>	66.1 <sub>↑0.6</sub>
<b>Unstructured + Captioning</b>											
- BM25	40.1	38.4	70.0	35.4	61.5	60.9	88.0	84.7	82.7	89.2	65.1
- BGE-M3	35.7 <sub>↓4.4</sub>	32.9 <sub>↓5.4</sub>	71.9 <sub>↑1.9</sub>	69.1 <sub>↑33.7</sub>	43.8 <sub>↓17.7</sub>	73.1 <sub>↑12.2</sub>	88.8 <sub>↑0.8</sub>	83.3 <sub>↓1.4</sub>	80.4 <sub>↓2.3</sub>	91.3 <sub>↑2.1</sub>	67.0 <sub>↑1.9</sub>
<b>Contrastive VLMs</b>											
Jina-CLIP	25.4	11.9	35.5	20.2	3.3	3.8	15.2	19.7	21.4	20.8	17.7
Nomic-vision	17.1	10.7	30.1	16.3	2.7	1.1	12.9	10.9	11.4	15.7	12.9
SigLIP (Vanilla)	43.2	30.3	64.1	58.1	26.2	18.7	62.5	65.7	66.1	79.1	51.4
<b>Ours</b>											
SigLIP (Vanilla)	43.2	30.3	64.1	58.1	26.2	18.7	62.5	65.7	66.1	79.1	51.4
BiSigLIP (+fine-tuning)	58.5 <sub>↑15.3</sub>	32.9 <sub>↑2.6</sub>	70.5 <sub>↑6.4</sub>	62.7 <sub>↑4.6</sub>	30.5 <sub>↑4.3</sub>	26.5 <sub>↑7.8</sub>	74.3 <sub>↑11.8</sub>	73.7 <sub>↑8.0</sub>	74.2 <sub>↑8.1</sub>	82.3 <sub>↑3.2</sub>	58.6 <sub>↑7.2</sub>
BiPali (+LLM)	56.5 <sub>↓2.0</sub>	30.0 <sub>↓2.9</sub>	67.4 <sub>↓3.1</sub>	76.9 <sub>↑14.2</sub>	33.4 <sub>↑2.9</sub>	43.7 <sub>↑17.2</sub>	71.2 <sub>↓3.1</sub>	61.9 <sub>↓11.7</sub>	73.8 <sub>↓0.4</sub>	73.6 <sub>↓8.8</sub>	58.8 <sub>↑0.2</sub>
<i>ColPali</i> (+Late Inter.)	<b>79.1</b> <sub>↑22.6</sub>	<b>54.4</b> <sub>↑24.5</sub>	<b>81.8</b> <sub>↑14.4</sub>	<b>83.9</b> <sub>↑7.0</sub>	<b>65.8</b> <sub>↑32.4</sub>	<b>73.2</b> <sub>↑29.5</sub>	<b>96.2</b> <sub>↑25.0</sub>	<b>91.0</b> <sub>↑29.1</sub>	<b>92.7</b> <sub>↑18.9</sub>	<b>94.4</b> <sub>↑20.8</sub>	<b>81.3</b> <sub>↑22.5</sub>

Table 2: **Comprehensive evaluation of baseline models and our proposed method on ViDoRe.** Results are presented using nDCG@5 metrics, and illustrate the impact of different components. Text-only metrics are not computed for benchmarks with only visual elements.

## 5.1 PERFORMANCE (R1)

We show performance is achieved iteratively through the combination of three factors; (1) a carefully crafted task-specific dataset, (2) pairing a pretrained LLM to a vision model to better leverage text semantics from the image, and (3) using multi-vector embeddings rather than a single vector representation to better capture the vast amount of visual information present in a document.

**Fine-tuning a Vision Model on a document retrieval oriented dataset: *BiSigLIP*.** SigLIP<sup>9</sup> is a strong vision-language bi-encoder producing single vector embeddings, and pretrained on billions of image-text pairs from the English split of WebLI (Chen et al., 2023). Further fine-tuning the textual component of this model on our document-oriented dataset (BiSigLIP) yields clear improvements across the board, particularly on figure retrieval (ArxivQA) and table retrieval tasks (TabFQuAD).

**Feeding image patches to a LLM: *BiPali*.** In the PaliGemma model architecture, SigLIP-generated patch embeddings are fed to a text language model and we can obtain LLM contextualized output patch embeddings.<sup>10</sup> This technique aligns the image token representations with the text token embeddings in the LLM’s embeddings space, and augments the vision model embeddings with the language model’s text understanding capabilities. We average pool these representations to obtain a single dense vector, effectively creating a PaliGemma bi-encoder model (BiPali). After fine-tuning on the training dataset, we obtain a model that performs slightly worse in English than the tuned BiSigLIP variant.<sup>11</sup> However, we see notable improvements in French tasks, indicating that BiPali’s LLM (Gemma 2B) helps multilingual text understanding. This is particularly notable as our training dataset does not contain non-English samples.

**Leveraging Multi-Vector Embeddings through Late Interaction: *ColPali*.** One benefit of inputting image patch embeddings through a language model is that they are natively mapped to a latent space similar to the textual input (query). This enables leveraging the ColBERT strategy to construct one

<sup>9</sup><https://huggingface.co/google/siglip-so400m-patch14-384>

<sup>10</sup>Note that the SigLIP model used in PaliGemma slightly differs in terms of number patches - 1024 patches for PaliGemma’s vision encoder, and 729 for the standalone SigLIP model.

<sup>11</sup>This can be explained by the fact that contrary to SigLIP, the original PaliGemma is not trained on contrastive matching tasks, but rather on next token prediction. Our contrastive fine-tuning phase on 119K images to transform PaliGemma into a bi-encoder is 5 orders of magnitude smaller than SigLIP’s original contrastive training.

embedding per image patch token, and at inference compute **all** interactions between text tokens and image patches, resulting in a step-change improvement in performance compared to BiPali. Results in Table 2 show that our *ColPali* model also largely outperforms the strong baselines based on Unstructured and captioning, as well as all evaluated text-image embedding models. The difference is particularly stark on the more visually complex benchmark tasks, such as InfographicVQA, ArxivQA, and TabFQuAD, respectively representing infographics, figures, and tables. However, text-centric documents are also better retrieved by the *ColPali* models across all evaluated domains and languages, making our approach the overall best-performing document-retrieval model.

**Negative Results.** For extensiveness, we also train ColSigLIP, a late interaction variant of the BiSigLIP model but obtain abysmal performances. We attribute this to the large gaps w.r.t. SigLIP’s pre-training, in which only a pooled latent representation is used in the contrastive loss, which does not optimize the representations of individual patch and token embeddings. Similarly, we train a BiSigLIP<sub>PaliGemma</sub> variant, in which we retrieve the image representations from the SigLIP model that has been further updated by PaliGemma fine-tuning, and use the text representations from PaliGemma’s text model. After fine-tuning on our dataset, performance is severely inferior to SigLIP<sub>Vanilla</sub> which simply encodes with SigLIP’s original text and vision components. This indicates a logical misalignment between SigLIP embeddings, and Gemma embeddings after PaliGemma training. We detail these results in subsection C.1.

## 5.2 LATENCIES & MEMORY FOOTPRINT

**Online Querying. (R2)** Logically, querying latencies differ between *ColPali* and a BGE-M3 embedding model. For BGE, encoding takes about 22 ms for 15 tokens, while encoding a query with *ColPali*’s language model takes about 30 ms<sup>12</sup>. For smaller corpus sizes, computing the late interaction operation induces marginally small overheads ( $\approx 1$  ms per 1000 pages in the corpus), and the cosine similarity computation between bi-encoder vectors is even faster. Optimized late interaction engines (Santhanam et al., 2022; Lee et al., 2023) enable to easily scale corpus sizes to millions of documents with reduced latency degradations.

**Offline Indexing. (R3)** Standard retrieval methods using bi-encoders represent each chunk as a single vector embedding, which is easy to store and fast to compute. However, processing a PDF to get the different chunks is the most time-consuming part (layout detection, OCR, chunking), and using captioning to handle multimodal data will only exacerbate this already lengthy process. On the other hand, *ColPali* directly encodes pages from their image representation. Although the model is larger than standard retrieval encoders, skipping the preprocessing allows large speedups at indexing<sup>13</sup> (Figure 2). As pages are embedded end-to-end in single forward pass, the VRAM usage depends exclusively on the sequence length (number of patches per image) which is fixed as well, enabling efficient batching strategies to fully leverage hardware acceleration. ColPali also benefits from most LLM efficiency improvements introduced in the ecosystem such as Flash Attention (Dao, 2023).

**Storage Footprint.** Our method requires storing a vector per image patch, along with 6 extra text tokens “Describe the image” concatenated to image patches. We project each PaliGemma vector to a lower dimensional space ( $D = 128$ ) to maximize efficiency, leading to a memory footprint of 257.5 KB per page (subsection B.3). Importantly, the memory footprint of the naive ColBERT indexing strategy can be drastically improved through compression and clustering mechanisms (Santhanam et al., 2022; Clavié et al., 2024).

**Token pooling.** Token pooling (Clavié et al., 2024) is a CRUDE-compliant method (document addition/deletion-friendly) that aims to reduce the amount of multi-vector embeddings. For ColPali, many image patches share redundant information, e.g. white background patches. By pooling these patches together, we can reduce the amount of embeddings while retaining most information. Retrieval performance with hierarchical mean token pooling on image embeddings is shown in Figure 3 (left). With a pool factor of 3, the total number of vectors is reduced by 66.7% while 97.8% of the original performance is maintained. We note that the Shift dataset - composed of the most text-dense documents - is a clear outlier, showcasing more information dense documents contain less redundant patches and may be prone to worse performance degradation with such pooling techniques.

<sup>12</sup>Computed for a batch size of 1 (online), and averaged over 1000 queries. See subsection B.4

<sup>13</sup>Measures a NVIDIA L4 GPU, averaged on 100 pages, with a batch size of 4 pages for *ColPali* and 8 text chunks for Bi-Encoders. On average, a page is divided into 2.1 chunks. See subsection B.4.



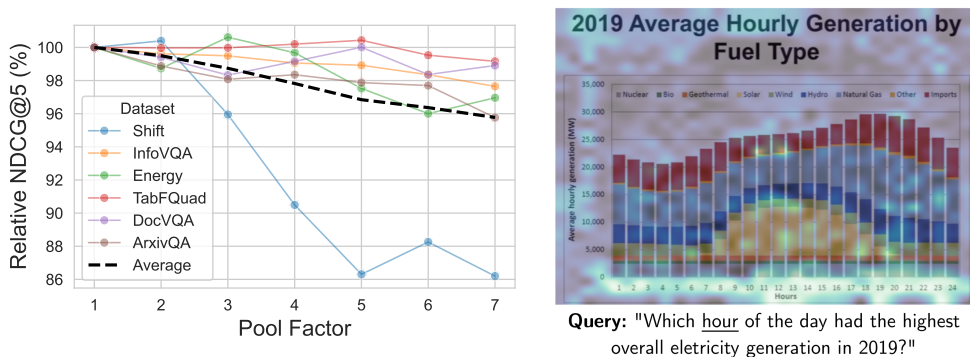


Figure 3: (Left: **Token Pooling**) Relative performance degradation when reducing the number of stored embeddings per document. (Right: **Interpretability**) For each term in a user query, *ColPali* identifies the most relevant document image patches (highlighted zones) and computes a query-to-page matching score.

### 5.3 INTERPRETABILITY

By superimposing the late interaction heatmap on top of the original image, we can visualize the most salient image patches with respect to each term of the query, yielding interpretable insights into model focus zones. As epitomized in Figure 3 (right), we observe *ColPali* exhibits strong OCR capabilities as both the words “hourly” and “hours” present a high similarity score with the query token `<.hour>`. We also note particular focus on other non-trivial image features such as the x-axis representing hours being salient. Other visualization examples are shown in Appendix D.

## 6 ABLATION STUDY

We run various ablations to better understand the mechanisms at play. By default, result deltas reported below refer to nDCG@5 values averaged over all ViDoRe tasks. Detailed results in C.2.

**Tradeoffs between model size and the number of image patches.** We train a variant of PaliGemma with half the number of image patches (512). While we observe a clear performance degradation with respects to to the 1024-patch *ColPali* model ( $-24.8$  nDCG@5), memory usage is much lower. As an alternative to PaliGemma, we train Idefics2-8B (Laurençon et al., 2024b), a VLM with a similar architecture and based on a Mistral-7B (Jiang et al., 2023) language backbone and a SigLIP vision encoder paired with a perceiver resampler. The most notable differences with PaliGemma lie in the size of the language model (2B and 7B resp.) and the number of image patches (between 512 and 2048 for PaliGemma, and 64 post-resampling for Idefics2<sup>14</sup>). Our results suggest better language models enable more efficient representations of image embeddings - ColIdefics2 with 64 patches largely outperforms out *ColPali* with 512 patches ( $+20.1$  nDCG@5). However ColIdefics2 (64) remains less accurate than ColPali (1024) ( $-4.7$  nDCG@5) while being about twice as slow in terms of training and inference latency. These results suggest there are *tradeoffs* between performance (R1), latencies during online querying (R2) and offline indexation phases (R3), and index memory size.

**Unfreezing the vision component.** We train a *ColPali* variant by also backpropagating through and updating the vision encoder and the projection layer. This leads to a slight performance degradation ( $-0.7$  nDCG@5). These conclusions may change with larger scales of training data.

**Impact of “query augmentation” tokens.** In ColBERT, special tokens are concatenated to the input query to serve as soft query augmentation buffers. Training without these tokens, we observe no significant performance difference in the English benchmarks. However, performance on the French tasks seems to improve ( $+9.8$  nDCG@G on Shift,  $+6.3$  nDCG@5 on TabFQuAD, Table 7).

**Impact of the Pairwise CE loss.** Training with an in-batch negative contrastive loss, instead of the pairwise CE loss that only considers the hardest negative sample, leads to a slight performance degradation ( $-1.6$  nDCG@5) on the aggregated benchmark.

<sup>14</sup>With the option of adding 4 sub-image crops of 64 tokens each to the sequence, for a total of 320 tokens

**Adapting models to new tasks.** Contrary to more complex multi-step retrieval pipelines, *ColPali* can be trained end-to-end, directly optimizing the downstream retrieval task which greatly facilitates fine-tuning to boost performance on specialized domains, multilingual retrieval, or specific visual elements the model struggles with. To demonstrate, we add 1552 samples representing French tables and associated queries to the training set. This represents the only French data in the training set, with all other examples being kept unchanged. We see clear nDCG@5 improvements (+2.6) and even starker Recall@1 gains (+5) on the TabFQuAD benchmark, with no performance degradation on the rest of the benchmark tasks (+0.4 nDCG@5 overall).

**Better VLMs lead to better visual retrievers.** As improved VLMs are released, it is interesting to observe if improved performances on generative tasks translate once these models are adapted for image retrieval tasks through ColPali training strategies. We train the recently released Qwen2-VL 2B (Wang et al., 2024b), a SOTA 2 billion parameter generative VLM, with the same data and training strategy, obtaining ColQwen2-VL. To approximately match ColPali’s memory requirements, we limit the number of image patches to 768, slightly less than ColPali’s 1024 patches. We observe clear performance improvements of +5.3 nDCG@5 values over ColPali showcasing clear performance correlations between generative benchmarks performance and retrieving metrics.

**Out-of-domain generalization.** Some of the datasets in the ViDoRe benchmark have train sets, which we have integrated within the ColPali train set (eg. academic tasks). This is standard in embedding models (Wang et al., 2024a; Lee et al., 2024), and while ColPali also exhibits strong performance on tasks in which this is not the case (French data is never seen by the model during training for instance), it remains interesting to evaluate model performance when training is done on a fully disjoint data distribution. We train a ColPali variant solely using the recent DocMatix dataset (Laurençon et al., 2024a), a large scale, synthetically annotated visual document question answering dataset, which we subsample to obtain a comparably-sized train set. Results on ViDoRe show the performance drop is minor (−2.2 nDCG@5), still outperforming the closest baseline method by over 12 points. These results showcase ColPali generalizes well outside of its training distribution, and demonstrate that our results are not unreasonably boosted with respect to baselines (BGE-M3) that cannot be fine-tuned on the same data<sup>15</sup>

## 7 CONCLUSIONS

In this work, we introduced the Visual Document Retrieval Benchmark (*ViDoRe*), which evaluates document retrieval systems in realistic settings involving visually complex documents. We demonstrated that current retrieval pipelines and contrastive vision-language models struggle to efficiently exploit visual information embedded in documents, leading to suboptimal performance. To address this, we presented *ColPali*, a novel retrieval method that leverages Vision-Language Models to create high-quality, multi-vector embeddings purely from visual document features. *ColPali* largely outperforms the best existing document retrieval methods while enabling faster corpus indexing times and maintaining low querying latencies, thus circumventing many pain points of modern document retrieval applications. We hope to drive industrial adoption, and to encourage future work by publicly releasing the *ViDoRe* benchmark, the data, the codebase, and all models and baselines from our work.

**Future Work.** Beyond performance improvements that could be obtained through better data, backbone models or training strategies, our vision at term is to combine visual retrieval systems and visually grounded query answering to create end-to-end RAG systems that purely function from image features. This idea is supported by concurrent work (Ma et al., 2024) showcasing the strong promises of VLMs for visual QA, and may eventually become a new industrial standard for document processing. In this line of work, reliability is key, and confidence estimation techniques for Information Retrieval methods could become central to implement abstention mechanisms (Gisserot-Boukhlef et al., 2024), and are particularly interesting given the information rich multi-vector scoring mechanisms of late interaction systems. **Expanding benchmarking efforts to cover more languages, modalities, and tasks is also a crucial future research direction (Jiang et al., 2024).**

<sup>15</sup>To train with data resembling the one BGE-M3 models would see at inference time would require running complex extraction pipelines for the more than 100K documents in the training set, notably relying on external proprietary captioning models which is both too costly and lengthy. This is not needed to train vision-based models.

540 REPRODUCIBILITY STATEMENT

541  
542 For transparency, reproducibility and to foster future work, we release our training data, model  
543 checkpoints (adapters), entire codebase, and complete evaluation benchmark under MIT licenses as  
544 detailed in the main paper. We also host a public ViDoRe leaderboard<sup>16</sup> to foster concurrent work in  
545 the space. The supplementary material further details training configurations for our models (also  
546 specified in HuggingFace model repositories), and dives into the process we used to generate synthetic  
547 data, how latency computations are performed, as well as provides further detailed evaluation results.

548  
549 REFERENCES

550  
551 Ibrahim Alabdulmohsin, Xiaohua Zhai, Alexander Kolesnikov, and Lucas Beyer. Getting ViT in  
552 Shape: Scaling Laws for Compute-Optimal Model Design. 2023. doi: 10.48550/ARXIV.2305.  
553 13035. URL <https://arxiv.org/abs/2305.13035>. Publisher: arXiv Version Number: 5.

554 Jean-Baptiste Alayrac, Jeff Donahue, Pauline Luc, Antoine Miech, Iain Barr, Yana Hasson, Karel  
555 Lenc, Arthur Mensch, Katie Millican, Malcolm Reynolds, Roman Ring, Eliza Rutherford, Serkan  
556 Cabi, Tengda Han, Zhitao Gong, Sina Samangooei, Marianne Monteiro, Jacob Menick, Sebastian  
557 Borgeaud, Andrew Brock, Aida Nematzadeh, Sahand Sharifzadeh, Mikolaj Binkowski, Ricardo  
558 Barreira, Oriol Vinyals, Andrew Zisserman, and Karen Simonyan. Flamingo: a Visual Language  
559 Model for Few-Shot Learning. 2022. doi: 10.48550/ARXIV.2204.14198. URL <https://arxiv.org/abs/2204.14198>. Publisher: arXiv Version Number: 2.

560  
561 Anthropic. The Claude 3 Model Family: Opus, Sonnet, Haiku, 2024. URL  
562 [https://www-cdn.anthropic.com/de8ba9b01c9ab7cbabf5c33b80b7bbc618857627/](https://www-cdn.anthropic.com/de8ba9b01c9ab7cbabf5c33b80b7bbc618857627/Model_Card_Claude_3.pdf)  
563 [Model\\_Card\\_Claude\\_3.pdf](https://www-cdn.anthropic.com/de8ba9b01c9ab7cbabf5c33b80b7bbc618857627/Model_Card_Claude_3.pdf).

564  
565 Srikar Appalaraju, Bhavan Jasani, Bhargava Urala Kota, Yusheng Xie, and R. Manmatha. DocFormer:  
566 End-to-End Transformer for Document Understanding, 2021. URL [https://arxiv.org/abs/](https://arxiv.org/abs/2106.11539)  
567 [2106.11539](https://arxiv.org/abs/2106.11539). Version Number: 2.

568 Jinze Bai, Shuai Bai, Shusheng Yang, Shijie Wang, Sinan Tan, Peng Wang, Junyang Lin, Chang  
569 Zhou, and Jingren Zhou. Qwen-VL: A Versatile Vision-Language Model for Understanding,  
570 Localization, Text Reading, and Beyond. 2023. doi: 10.48550/ARXIV.2308.12966. URL  
571 <https://arxiv.org/abs/2308.12966>. Publisher: arXiv Version Number: 3.

572  
573 Payal Bajaj, Daniel Campos, Nick Craswell, Li Deng, Jianfeng Gao, Xiaodong Liu, Rangan Ma-  
574 jumder, Andrew McNamara, Bhaskar Mitra, Tri Nguyen, Mir Rosenberg, Xia Song, Alina Stoica,  
575 Saurabh Tiwary, and Tong Wang. MS MARCO: A Human Generated MACHine Reading COMpre-  
576 hension Dataset, 2016. URL <https://arxiv.org/abs/1611.09268>. Version Number: 3.

577 Lucas Beyer, Andreas Steiner, André Susano Pinto, Alexander Kolesnikov, Xiao Wang, Daniel Salz,  
578 Maxim Neumann, Ibrahim Alabdulmohsin, Michael Tschannen, Emanuele Bugliarello, Thomas  
579 Unterthiner, Daniel Keysers, Skanda Koppula, Fangyu Liu, Adam Grycner, Alexey Gritsenko,  
580 Neil Houlsby, Manoj Kumar, Keran Rong, Julian Eisenschlos, Rishabh Kabra, Matthias Bauer,  
581 Matko Bošnjak, Xi Chen, Matthias Minderer, Paul Voigtlaender, Ioana Bica, Ivana Balazevic, Joan  
582 Puigcerver, Pinelopi Papalampidi, Olivier Henaff, Xi Xiong, Radu Soricut, Jeremiah Harmsen,  
583 and Xiaohua Zhai. Paligemma: A versatile 3b vlm for transfer, 2024. URL [https://arxiv.org/](https://arxiv.org/abs/2407.07726)  
584 [abs/2407.07726](https://arxiv.org/abs/2407.07726).

585  
586 Burton H. Bloom. Space/time trade-offs in hash coding with allowable errors. *Commun. ACM*, 13(7):  
587 422–426, July 1970. ISSN 0001-0782. doi: 10.1145/362686.362692. URL [https://doi.org/](https://doi.org/10.1145/362686.362692)  
588 [10.1145/362686.362692](https://doi.org/10.1145/362686.362692). Place: New York, NY, USA Publisher: Association for Computing  
589 Machinery.

589 Łukasz Borchmann, Michał Pietruszka, Tomasz Stanislawek, Dawid Jurkiewicz, Michał Turski,  
590 Karolina Szyndler, and Filip Galiński. DUE: End-to-End Document Understanding Benchmark.  
591 In *Thirty-fifth Conference on Neural Information Processing Systems Datasets and Benchmarks*  
592 *Track (Round 2)*, 2021. URL <https://openreview.net/forum?id=rNs2FvJGDK>.

593  
<sup>16</sup>[https://huggingface.co/spaces/\(anonymous\)](https://huggingface.co/spaces/(anonymous))

- 594 Jianlv Chen, Shitao Xiao, Peitian Zhang, Kun Luo, Defu Lian, and Zheng Liu. BGE M3-Embedding:  
595 Multi-Lingual, Multi-Functionality, Multi-Granularity Text Embeddings Through Self-Knowledge  
596 Distillation, 2024. URL <https://arxiv.org/abs/2402.03216>. Version Number: 3.  
597
- 598 Xi Chen, Xiao Wang, Lucas Beyer, Alexander Kolesnikov, Jialin Wu, Paul Voigtlaender, Basil  
599 Mustafa, Sebastian Goodman, Ibrahim Alabdulmohsin, Piotr Padlewski, Daniel Salz, Xi Xiong,  
600 Daniel Vlasic, Filip Pavetic, Keran Rong, Tianli Yu, Daniel Keysers, Xiaohua Zhai, and Radu  
601 Soricut. PaLI-3 Vision Language Models: Smaller, Faster, Stronger, 2023. URL <https://arxiv.org/abs/2310.09199>. Version Number: 2.  
602
- 603 Benjamin Clavié, Antoine Chaffin, and Griffin Adams. Reducing the Footprint of Multi-Vector  
604 Retrieval with Minimal Performance Impact via Token Pooling, 2024. URL <https://arxiv.org/abs/2409.14683>. Version Number: 1.  
605
- 606  
607 Cohere. Introducing Rerank 3: A New Foundation Model for Efficient Enterprise Search & Retrieval,  
608 April 2024. URL <https://cohere.com/blog/rerank-3>.
- 609 Tri Dao. Flashattention-2: Faster attention with better parallelism and work partitioning, 2023. URL  
610 <https://arxiv.org/abs/2307.08691>.  
611
- 612 Timothée Darcet, Maxime Oquab, Julien Mairal, and Piotr Bojanowski. Vision Transformers Need  
613 Registers. 2023. doi: 10.48550/ARXIV.2309.16588. URL <https://arxiv.org/abs/2309.16588>.  
614 16588. Publisher: [object Object] Version Number: 2.
- 615 Jacob Devlin, Ming-Wei Chang, Kenton Lee, and Kristina Toutanova. BERT: Pre-training of Deep  
616 Bidirectional Transformers for Language Understanding, 2018. URL <https://arxiv.org/abs/1810.04805>. Version Number: 2.  
617
- 618  
619 Alexey Dosovitskiy, Lucas Beyer, Alexander Kolesnikov, Dirk Weissenborn, Xiaohua Zhai, Thomas  
620 Unterthiner, Mostafa Dehghani, Matthias Minderer, Georg Heigold, Sylvain Gelly, Jakob Uszkoreit,  
621 and Neil Houlsby. An Image is Worth 16x16 Words: Transformers for Image Recognition at  
622 Scale. 2020. doi: 10.48550/ARXIV.2010.11929. URL <https://arxiv.org/abs/2010.11929>.  
623 Publisher: arXiv Version Number: 2.
- 624 Zheng Ge, Songtao Liu, Feng Wang, Zeming Li, and Jian Sun. YOLOX: Exceeding YOLO Series in  
625 2021, 2021. URL <https://arxiv.org/abs/2107.08430>. Version Number: 2.  
626
- 627 Gemma Team, Thomas Mesnard, Cassidy Hardin, Robert Dadashi, Surya Bhupatiraju, Shreya Pathak,  
628 Laurent Sifre, Morgane Rivière, Mihir Sanjay Kale, Juliette Love, Pouya Tafti, Léonard Hussenot,  
629 Pier Giuseppe Sessa, Aakanksha Chowdhery, Adam Roberts, Aditya Barua, Alex Botev, Alex  
630 Castro-Ros, Ambrose Slone, Amélie Héliou, Andrea Tacchetti, Anna Bulanova, Antonia Paterson,  
631 Beth Tsai, Bobak Shahriari, Charline Le Lan, Christopher A. Choquette-Choo, Clément Crepy,  
632 Daniel Cer, Daphne Ippolito, David Reid, Elena Buchatskaya, Eric Ni, Eric Noland, Geng Yan,  
633 George Tucker, George-Christian Muraru, Grigory Rozhdestvenskiy, Henryk Michalewski, Ian  
634 Tenney, Ivan Grishchenko, Jacob Austin, James Keeling, Jane Labanowski, Jean-Baptiste Lespiau,  
635 Jeff Stanway, Jenny Brennan, Jeremy Chen, Johan Ferret, Justin Chiu, Justin Mao-Jones, Katherine  
636 Lee, Kathy Yu, Katie Millican, Lars Lowe Sjoesund, Lisa Lee, Lucas Dixon, Machel Reid, Maciej  
637 Michał, Mateo Wirth, Michael Sharman, Nikolai Chirukov, Nithum Thain, Olivier Bachem, Oscar  
638 Chang, Oscar Wahltinez, Paige Bailey, Paul Michel, Petko Yotov, Rahma Chaabouni, Ramona  
639 Comanescu, Reena Jana, Rohan Anil, Ross McIlroy, Ruibo Liu, Ryan Mullins, Samuel L Smith,  
640 Sebastian Borgeaud, Sertan Girgin, Sholto Douglas, Shree Pandya, Siamak Shakeri, Soham De,  
641 Ted Klimentko, Tom Hennigan, Vlad Feinberg, Wojciech Stokowiec, Yu-hui Chen, Zafarali Ahmed,  
642 Zhitao Gong, Tris Warkentin, Ludovic Peran, Minh Giang, Clément Farabet, Oriol Vinyals, Jeff  
643 Dean, Koray Kavukcuoglu, Demis Hassabis, Zoubin Ghahramani, Douglas Eck, Joelle Barral,  
644 Fernando Pereira, Eli Collins, Armand Joulin, Noah Fiedel, Evan Senter, Alek Andreev, and  
645 Kathleen Kenealy. Gemma: Open Models Based on Gemini Research and Technology, 2024. URL  
646 <https://arxiv.org/abs/2403.08295>. Version Number: 4.  
647
- 648 Hippolyte Gisserot-Boukhlef, Manuel Faysse, Emmanuel Malherbe, Céline Hudelot, and Pierre  
649 Colombo. Towards trustworthy reranking: A simple yet effective abstention mechanism, 2024.  
650 URL <https://arxiv.org/abs/2402.12997>.

- 648 Edward J. Hu, Yelong Shen, Phillip Wallis, Zeyuan Allen-Zhu, Yuanzhi Li, Shean Wang, Lu Wang,  
649 and Weizhu Chen. LoRA: Low-Rank Adaptation of Large Language Models. 2021. doi: 10.48550/  
650 ARXIV.2106.09685. URL <https://arxiv.org/abs/2106.09685>. Publisher: arXiv Version  
651 Number: 2.
- 652 Yupan Huang, Tengchao Lv, Lei Cui, Yutong Lu, and Furu Wei. LayoutLMv3: Pre-training for  
653 Document AI with Unified Text and Image Masking. 2022. doi: 10.48550/ARXIV.2204.08387.  
654 URL <https://arxiv.org/abs/2204.08387>. Publisher: arXiv Version Number: 3.
- 656 Albert Q. Jiang, Alexandre Sablayrolles, Arthur Mensch, Chris Bamford, Devendra Singh Chaplot,  
657 Diego de las Casas, Florian Bressand, Gianna Lengyel, Guillaume Lample, Lucile Saulnier,  
658 L elio Renard Lavaud, Marie-Anne Lachaux, Pierre Stock, Teven Le Scao, Thibaut Lavril, Thomas  
659 Wang, Timoth e Lacroix, and William El Sayed. Mistral 7B. 2023. doi: 10.48550/ARXIV.2310.  
660 06825. URL <https://arxiv.org/abs/2310.06825>. Publisher: arXiv Version Number: 1.
- 661 Ziyang Jiang, Rui Meng, Xinyi Yang, Semih Yavuz, Yingbo Zhou, and Wenhua Chen. Vlm2vec:  
662 Training vision-language models for massive multimodal embedding tasks, 2024. URL <https://arxiv.org/abs/2410.05160>.
- 665 Vladimir Karpukhin, Barlas O uz, Sewon Min, Patrick Lewis, Ledell Wu, Sergey Edunov, Danqi  
666 Chen, and Wen-tau Yih. Dense Passage Retrieval for Open-Domain Question Answering, 2020.  
667 URL <https://arxiv.org/abs/2004.04906>. Version Number: 3.
- 668 Omar Khattab and Matei Zaharia. ColBERT: Efficient and Effective Passage Search via Con-  
669 textualized Late Interaction over BERT. 2020. doi: 10.48550/ARXIV.2004.12832. URL  
670 <https://arxiv.org/abs/2004.12832>.
- 672 Geewook Kim, Teakgyu Hong, Moonbin Yim, Jeongyeon Nam, Jinyoung Park, Jinyeong Yim,  
673 Wonseok Hwang, Sangdoon Yun, Dongyoon Han, and Seunghyun Park. OCR-free Document Un-  
674 derstanding Transformer, 2021. URL <https://arxiv.org/abs/2111.15664>. Version Number:  
675 5.
- 676 Andreas Koukounas, Georgios Mastrapas, Michael G unther, Bo Wang, Scott Martens, Isabelle Mohr,  
677 Saba Sturua, Mohammad Kalim Akram, Joan Fontanals Mart nez, Saahil Ognawala, Susana  
678 Guzman, Maximilian Werk, Nan Wang, and Han Xiao. Jina CLIP: Your CLIP Model Is Also Your  
679 Text Retriever, 2024. URL <https://arxiv.org/abs/2405.20204>. Version Number: 1.
- 681 Hugo Lauren on, Andr s Marafioti, Victor Sanh, and L eo Tronchon. Building and better understand-  
682 ing vision-language models: insights and future directions., 2024a.
- 683 Hugo Lauren on, L eo Tronchon, Matthieu Cord, and Victor Sanh. What matters when building vision-  
684 language models?, May 2024b. URL <http://arxiv.org/abs/2405.02246>. arXiv:2405.02246  
685 [cs].
- 687 Chankyu Lee, Rajarshi Roy, Mengyao Xu, Jonathan Raiman, Mohammad Shoeybi, Bryan Catanzaro,  
688 and Wei Ping. Nv-embed: Improved techniques for training llms as generalist embedding models,  
689 2024. URL <https://arxiv.org/abs/2405.17428>.
- 690 Jinhyuk Lee, Zhuyun Dai, Sai Meher Karthik Duddu, Tao Lei, Iftekhar Naim, Ming-Wei Chang, and  
691 Vincent Y. Zhao. Rethinking the Role of Token Retrieval in Multi-Vector Retrieval, 2023. URL  
692 <https://arxiv.org/abs/2304.01982>. Version Number: 3.
- 694 Lei Li, Yuqi Wang, Runxin Xu, Peiyi Wang, Xiachong Feng, Lingpeng Kong, and Qi Liu. Multimodal  
695 arxiv: A dataset for improving scientific comprehension of large vision-language models, 2024.
- 696 Tsung-Yi Lin, Michael Maire, Serge Belongie, Lubomir Bourdev, Ross Girshick, James Hays, Pietro  
697 Perona, Deva Ramanan, C. Lawrence Zitnick, and Piotr Doll ar. Microsoft COCO: Common  
698 Objects in Context, 2014. URL <https://arxiv.org/abs/1405.0312>. Version Number: 3.
- 700 Haotian Liu, Chunyuan Li, Qingyang Wu, and Yong Jae Lee. Visual Instruction Tuning. 2023. doi:  
701 10.48550/ARXIV.2304.08485. URL <https://arxiv.org/abs/2304.08485>. Publisher: arXiv  
Version Number: 1.

- 702 Lucas Beyer\*, Andreas Steiner\*, André Susano Pinto\*, Alexander Kolesnikov\*, Xiao Wang\*,  
703 Xiaohua Zhai\*, Daniel Salz, Maxim Neumann, Ibrahim Alabdulmohsin, Michael Tschannen,  
704 Jeremiah Harmsen, Daniel Keysers, Neil Houlsby, Xi Chen, Emanuele Bugliarello, Thomas  
705 Unterthiner, Keran Rong, Matthias Minderer, Ioana Bica, Ivana Balazevic, Joan Puigcerver, Julian  
706 Eisenschlos, Manoj Kumar, Matko Bošnjak, Matthias Bauer, Fangyu Liu, Adam Grycner, Alexey  
707 Gritsenko, Paul Voigtlaender, Pinelopi Papalampidi, Olivier Henaff, Skanda Koppula, Xi Xiong,  
708 Radu Soricut, Model release contributors and general support, Tris Warkentin, Kat Black, Luiz  
709 Gustavo Martins, Glenn Cameron, Raj Gundluru, Manvinder Singh, Meg Risdal, Nilay Chauhan,  
710 Nate Keating, Nesh Devanathan, Elisa Bandy, Joe Fernandez, Antonia Paterson, Jenny Brennan,  
711 Tom Eccles, Pankil Botadra, Ben Bariach, Lav Rai, Minwoo Park, Dustin Luong, Daniel Vlasic,  
712 Bo Wu, Wenming Ye, Divyashree Sreepathihalli, Kiranbir Sodhia, Alek Andreev, Armand Joulin,  
713 Surya Bhupatiraju, Minh Giang, Joelle Barral, and Zoubin Ghahramani. PaliGemma, 2024. URL  
714 <https://www.kaggle.com/m/23393>.
- 715 Yubo Ma, Yuhang Zang, Liangyu Chen, Meiqi Chen, Yizhu Jiao, Xinze Li, Xinyuan Lu, Ziyu  
716 Liu, Yan Ma, Xiaoyi Dong, Pan Zhang, Liangming Pan, Yu-Gang Jiang, Jiaqi Wang, Yixin Cao,  
717 and Aixin Sun. Mmlongbench-doc: Benchmarking long-context document understanding with  
718 visualizations, 2024. URL <https://arxiv.org/abs/2407.01523>.
- 719 Minesh Mathew, Dimosthenis Karatzas, and C. V. Jawahar. DocVQA: A Dataset for VQA on  
720 Document Images. 2020. doi: 10.48550/ARXIV.2007.00398. URL <https://arxiv.org/abs/2007.00398>.
- 722 Minesh Mathew, Viraj Bagal, Rubèn Pérez Tito, Dimosthenis Karatzas, Ernest Valveny, and C. V.  
723 Jawahar. InfographicVQA, 2021. URL <https://arxiv.org/abs/2104.12756>. Version Number:  
724 2.
- 726 Niklas Muennighoff, Nouamane Tazi, Loïc Magne, and Nils Reimers. MTEB: Massive Text Embed-  
727 ding Benchmark, 2022. URL <https://arxiv.org/abs/2210.07316>. Version Number: 3.
- 728 Nomic. Nomic Embed Vision: Expanding The Nomic Latent Space, June 2024. URL <https://blog.nomic.ai/posts/nomic-embed-vision>.
- 731 Averi Nowak, Francesco Piccinno, and Yasemin Altun. Multimodal chart retrieval: A comparison  
732 of text, table and image based approaches. In Kevin Duh, Helena Gomez, and Steven Bethard  
733 (eds.), *Proceedings of the 2024 Conference of the North American Chapter of the Association  
734 for Computational Linguistics: Human Language Technologies (Volume 1: Long Papers)*, pp.  
735 5488–5505, Mexico City, Mexico, June 2024. Association for Computational Linguistics. doi:  
736 10.18653/v1/2024.naacl-long.307. URL <https://aclanthology.org/2024.naacl-long.307>.
- 737 Alec Radford, Jong Wook Kim, Chris Hallacy, Aditya Ramesh, Gabriel Goh, Sandhini Agarwal,  
738 Girish Sastry, Amanda Askell, Pamela Mishkin, Jack Clark, Gretchen Krueger, and Ilya Sutskever.  
739 Learning Transferable Visual Models From Natural Language Supervision. 2021. doi: 10.48550/  
740 ARXIV.2103.00020. URL <https://arxiv.org/abs/2103.00020>. Publisher: arXiv Version  
741 Number: 1.
- 742 Nils Reimers and Iryna Gurevych. Sentence-BERT: Sentence Embeddings using Siamese BERT-  
743 Networks, 2019. URL <https://arxiv.org/abs/1908.10084>. Version Number: 1.
- 744 Stephen E. Robertson, Steve Walker, Susan Jones, Micheline Hancock-Beaulieu, and Mike Gatford.  
745 Okapi at TREC-3. In Donna K. Harman (ed.), *Proceedings of The Third Text REtrieval Conference,  
746 TREC 1994, Gaithersburg, Maryland, USA, November 2-4, 1994*, volume 500-225 of *NIST Special  
747 Publication*, pp. 109–126. National Institute of Standards and Technology (NIST), 1994. URL  
748 <http://trec.nist.gov/pubs/trec3/papers/city.ps.gz>.
- 749 Keshav Santhanam, Omar Khattab, Christopher Potts, and Matei Zaharia. PLAID: An Efficient  
750 Engine for Late Interaction Retrieval, 2022. URL <https://arxiv.org/abs/2205.09707>. Version  
751 Number: 1.
- 753 R. Smith. An Overview of the Tesseract OCR Engine. In *Ninth International Conference on  
754 Document Analysis and Recognition (ICDAR 2007) Vol 2*, pp. 629–633, Curitiba, Parana, Brazil,  
755 September 2007. IEEE. ISBN 978-0-7695-2822-9. doi: 10.1109/ICDAR.2007.4376991. URL  
<http://ieeexplore.ieee.org/document/4376991/>. ISSN: 1520-5363.

- 756 Karen Sparck Jones. A STATISTICAL INTERPRETATION OF TERM SPECIFICITY AND ITS  
757 APPLICATION IN RETRIEVAL. *Journal of Documentation*, 28(1):11–21, January 1972. ISSN  
758 0022-0418. doi: 10.1108/eb026526. URL [https://www.emerald.com/insight/content/doi/](https://www.emerald.com/insight/content/doi/10.1108/eb026526/full/html)  
759 [10.1108/eb026526/full/html](https://www.emerald.com/insight/content/doi/10.1108/eb026526/full/html).  
760
- 761 Zineng Tang, Ziyi Yang, Guoxin Wang, Yuwei Fang, Yang Liu, Chenguang Zhu, Michael Zeng, Cha  
762 Zhang, and Mohit Bansal. Unifying Vision, Text, and Layout for Universal Document Processing,  
763 2022. URL <https://arxiv.org/abs/2212.02623>. Version Number: 3.
- 764 Nandan Thakur, Nils Reimers, Andreas Rücklé, Abhishek Srivastava, and Iryna Gurevych. BEIR: A  
765 Heterogenous Benchmark for Zero-shot Evaluation of Information Retrieval Models, 2021. URL  
766 <https://arxiv.org/abs/2104.08663>. Version Number: 4.  
767
- 768 Ashish V. Thapliyal, Jordi Pont-Tuset, Xi Chen, and Radu Soricut. Crossmodal-3600: A Massively  
769 Multilingual Multimodal Evaluation Dataset, 2022. URL <https://arxiv.org/abs/2205.12522>.  
770 Version Number: 2.
- 771 Liang Wang, Nan Yang, Xiaolong Huang, Binxing Jiao, Linjun Yang, Daxin Jiang, Rangan Majumder,  
772 and Furu Wei. Text Embeddings by Weakly-Supervised Contrastive Pre-training, 2022. URL  
773 <https://arxiv.org/abs/2212.03533>. Version Number: 2.  
774
- 775 Liang Wang, Nan Yang, Xiaolong Huang, Linjun Yang, Rangan Majumder, and Furu Wei. Improving  
776 text embeddings with large language models, 2024a. URL [https://arxiv.org/abs/2401.](https://arxiv.org/abs/2401.00368)  
777 [00368](https://arxiv.org/abs/2401.00368).
- 778 Peng Wang, Shuai Bai, Sinan Tan, Shijie Wang, Zhihao Fan, Jinze Bai, Keqin Chen, Xuejing Liu,  
779 Jialin Wang, Wenbin Ge, Yang Fan, Kai Dang, Mengfei Du, Xuancheng Ren, Rui Men, Dayiheng  
780 Liu, Chang Zhou, Jingren Zhou, and Junyang Lin. Qwen2-vl: Enhancing vision-language model’s  
781 perception of the world at any resolution, 2024b. URL <https://arxiv.org/abs/2409.12191>.  
782
- 783 Wenhui Wang, Furu Wei, Li Dong, Hangbo Bao, Nan Yang, and Ming Zhou. MiniLM: Deep  
784 Self-Attention Distillation for Task-Agnostic Compression of Pre-Trained Transformers, April  
785 2020. URL <http://arxiv.org/abs/2002.10957>. arXiv:2002.10957 [cs].  
786
- 787 Lewei Yao, Runhui Huang, Lu Hou, Guansong Lu, Minzhe Niu, Hang Xu, Xiaodan Liang, Zhenguo  
788 Li, Xin Jiang, and Chunjing Xu. FILIP: Fine-grained Interactive Language-Image Pre-Training,  
789 2021. URL <https://arxiv.org/abs/2111.07783>. Version Number: 1.
- 790 Xiang Yue, Yuansheng Ni, Kai Zhang, Tianyu Zheng, Ruoqi Liu, Ge Zhang, Samuel Stevens, Dongfu  
791 Jiang, Weiming Ren, Yuxuan Sun, Cong Wei, Botao Yu, Ruibin Yuan, Renliang Sun, Ming Yin,  
792 Boyuan Zheng, Zhenzhu Yang, Yibo Liu, Wenhao Huang, Huan Sun, Yu Su, and Wenhao Chen.  
793 MMMU: A Massive Multi-discipline Multimodal Understanding and Reasoning Benchmark for  
794 Expert AGI, 2023. URL <https://arxiv.org/abs/2311.16502>. Version Number: 3.
- 795 Xiaohua Zhai, Basil Mustafa, Alexander Kolesnikov, and Lucas Beyer. Sigmoid Loss for Language  
796 Image Pre-Training. 2023. doi: 10.48550/ARXIV.2303.15343. URL [https://arxiv.org/abs/](https://arxiv.org/abs/2303.15343)  
797 [2303.15343](https://arxiv.org/abs/2303.15343). Publisher: [object Object] Version Number: 4.  
798
- 799 Li Zhang, Shuo Zhang, and Krisztian Balog. Table2vec: Neural word and entity embeddings for  
800 table population and retrieval. In *Proceedings of the 42nd International ACM SIGIR Conference*  
801 *on Research and Development in Information Retrieval*, SIGIR ’19. ACM, July 2019. doi:  
802 [10.1145/3331184.3331333](https://doi.org/10.1145/3331184.3331333). URL <http://dx.doi.org/10.1145/3331184.3331333>.
- 803 Ruochen Zhao, Hailin Chen, Weishi Wang, Fangkai Jiao, Xuan Long Do, Chengwei Qin, Bosheng  
804 Ding, Xiaobao Guo, Minzhi Li, Xingxuan Li, and Shafiq Joty. Retrieving Multimodal Information  
805 for Augmented Generation: A Survey, 2023. URL <https://arxiv.org/abs/2303.10868>.  
806 Version Number: 3.  
807
- 808 Fengbin Zhu, Wenqiang Lei, Fuli Feng, Chao Wang, Haozhou Zhang, and Tat-Seng Chua. Towards  
809 Complex Document Understanding By Discrete Reasoning. 2022. doi: 10.48550/ARXIV.2207.  
[11871](https://arxiv.org/abs/2207.11871). URL <https://arxiv.org/abs/2207.11871>. Publisher: arXiv Version Number: 3.

## 810 A BENCHMARK DATASETS

### 811 A.1 ACADEMIC DATASETS

812  
813  
814 **DocVQA** (Mathew et al., 2020) includes collected images from the UCSF Industry Documents  
815 Library. Questions and answers were manually annotated.

816  
817 **InfoVQA** (Mathew et al., 2021) includes infographics collected from the Internet using the search  
818 query “*infographics*”. Questions and answers were manually annotated.

819  
820 **TAT-DQA** (Zhu et al., 2022) is a large-scale Document VQA dataset that was constructed from  
821 publicly available real-world financial reports. It focuses on rich tabular and textual content requiring  
822 numerical reasoning. Questions and answers were manually annotated by human experts in finance.

823  
824 **arXivQA** (Li et al., 2024) is a VQA dataset based on figures extracted from arXiv publications. The  
825 questions were generated synthetically using GPT-4 Vision.

826  
827 **TabFQuAD** (Table French Question Answering Dataset) is designed to evaluate TableQA models  
828 in realistic industry settings. We create additional queries to augment the existing human-annotated  
829 ones using the same method described in subsection A.2.

### 830 A.2 PRACTICAL DATASETS

831  
832  
833 **Methodology.** Creating a relevant retrieval dataset close to real use cases is a major challenge as  
834 the dataset needs to be both sufficiently large for effective fine-tuning and sufficiently diverse to  
835 cover a broad range of modalities (full text, tables, charts, ...), domains (industry, healthcare, ...),  
836 and query-document interactions (extractive questions, open-ended questions, ...). Our approach to  
837 building this dataset involves several steps: (1) we use a web crawler to collect publicly available  
838 documents on various themes and sources, (2) we convert these PDFs into a series of images, one per  
839 page, and (3) we generate queries related to each image using a VLM.

840  
841 **Web-Crawler.** We implemented a web crawler to efficiently collect large volumes of documents  
842 related to a given topic. The crawler is seeded with a user-defined query (e.g. “artificial intelligence”)  
843 and then uses GPT-3.5 Turbo to brainstorm related topics and subtopics. This query augmentation  
844 strategy aims at both broadening and deepening the search. GPT-3.5 Turbo is further used to generate  
845 diverse search queries from each subtopic. This query set is then consumed by a pool of parallel  
846 workers whose job is to fetch the associated most relevant documents. We use SerpAPI<sup>17</sup> along with  
847 a filetype filter (PDF documents only) to programmatically scrape Google Search rankings. Each  
848 file is hashed and stored in a Bloom filter (Bloom, 1970) shared among workers to avoid duplicate  
849 documents in the final corpus. Unique scraped files are downloaded, and inserted into a SQLite  
850 database along with additional metadata.

851  
852 **Datamix.** Using the web crawler, we collected approximately 100 documents for each of the following  
853 four seeds: “*energy*”, “*government reports*”, “*healthcare industry*”, and “*artificial intelligence*”.  
854 These seeds were meticulously hand-picked to align with real-use cases for retrieval models and  
855 visually rich pages. We also removed all documents containing any private information.

856  
857 **Query Generation.** To increase the efficiency of our query generation scheme and to limit API calls,  
858 we generate at most 3 questions per image. From all the documents collected, we randomly sample  
859 10,000 images per theme and call Claude-3 Sonnet with the following prompt:

860  
861  
862  
863  

---

<sup>17</sup><https://serpapi.com/>



864  
865  
866  
867  
868  
869  
870  
871  
872  
873  
874  
875  
876  
877  
878  
879  
880  
881  
882  
883  
884  
885  
886  
887  
888  
889  
890  
891  
892  
893  
894  
895  
896  
897  
898  
899  
900  
901  
902  
903  
904  
905  
906  
907  
908  
909  
910  
911  
912  
913  
914  
915  
916  
917

You are an assistant specialized in Multimodal RAG tasks.

The task is the following: given an image from a pdf page, you will have to generate questions that can be asked by a user to retrieve information from a large documentary corpus.

The question should be relevant to the page, and should not be too specific or too general. The question should be about the subject of the page, and the answer needs to be found in the page.

Remember that the question is asked by a user to get some information from a large documentary corpus that contains multimodal data. Generate a question that could be asked by a user without knowing the existence and the content of the corpus.

Generate as well the answer to the question, which should be found in the page. And the format of the answer should be a list of words answering the question.

Generate at most THREE pairs of questions and answers per page in a dictionary with the following format, answer ONLY this dictionary NOTHING ELSE:

```
{
  "questions": [
    {
      "question": "XXXXXX",
      "answer": ["YYYYYY"]
    },
    {
      "question": "XXXXXX",
      "answer": ["YYYYYY"]
    },
    {
      "question": "XXXXXX",
      "answer": ["YYYYYY"]
    }
  ]
}
```

where XXXXXX is the question and ['YYYYYY'] is the corresponding list of answers that could be as long as needed.

Note: If there are no questions to ask about the page, return an empty list.

Focus on making relevant questions concerning the page.

Here is the page:

**Human Validation.** We manually validate every single synthetically created query in *ViDoRe* to ensure quality, query relevance, and consistency with the benchmark objective of evaluating retrieval in practical industrial settings. During this step, we randomly assign document-pair queries to 4 volunteer annotators and instruct them to filter out queries that do not fit the above-listed criteria. We also instruct annotators to flag any documents they deem to contain PII information or content not suited for an academic benchmark. No flag was raised during the entirety of the process, validating our prior PDF collection strategy. 100 queries per topic are collected in this manner. Annotators are colleagues and collaborators of the authors who volunteered to help. Each annotator spent approximately 3 hours filtering the larger query set down to 100 high-quality queries per topic.

### A.3 TRAINING DATASET

The statistics of the train set are given in the following table. The creation of the train set follows the same methodology as in subsection A.2. We made sure that a PDF document cannot have pages in both the training set and the test set to prevent data leakage and that there are no duplicate documents in each split.

Dataset Split	Split Size	Language	Domain
DocVQA	39,463	English	Scanned documents from UCSF Industry
InfoVQA	10,074	English	Infographics scrapped from the web
TATDQA	13,251	English	High-quality financial reports
arXivQA	10,000	English	Scientific Scientific Figures from arXiv
Scrapped PDFs	45,940	English	Varied PDFs from 3885 distinct URL domains
<b>TOTAL</b>	<b>118,695</b>	<b>English-only</b>	<b>Mixed</b>

Table 3: Details on the different splits in the dataset used to train ColPali.

## B IMPLEMENTATION DETAILS

### B.1 CODEBASE

The codebase is written in PyTorch<sup>18</sup> and leverages HuggingFace tooling for model implementations and trainers<sup>19</sup>.

### B.2 HYPERPARAMETERS

Hyperparameters are tuned on a validation split composed of 2% of the training dataset. We find bi-encoder methods to be more sensible to learning rate variations than late interaction-based models and achieve the best performance for all models with a learning rate of  $5e - 5$ . We experiment with LoRA rank and  $\alpha$  values and do not notice particular improvements past  $r = \alpha = 32$ . Per-device batch sizes are kept small due to long sequence lengths that complicate scaling past  $b = 4$ . We simulate larger batch sizes with multi-GPU training and train with a total batch size  $b = 32$  with no accumulation, for 1 epoch on our training set.

### B.3 EMBEDDING SIZE

Minimizing storage footprint can be essential to industrial retrieval systems if databases contain millions of documents. With this criterion in view, we have compared the embedding sizes of the models in our study. As shown in Table 4, *ColPali*'s embedding size is an order of magnitude larger than BM25 and two orders of magnitude larger than BGE-M3. However, in practical scenarios, pooling multi-vector embeddings by centroid cluster, or quantizing embeddings to binary representations<sup>20</sup> can reduce storage costs by two orders of magnitude (Santhanam et al., 2022) with minimal performance hits, and make storage costs competitive with other systems.

Model	Embedding size (KB)
BGE-M3	8.60
BM25 (dense emb.)	3.00
BM25 (sparse emb.)	$1.56 \pm 0.51$
<i>ColPali</i> (float16)	257.5

Table 4: Comparison of the embedding sizes for the DocVQA test set from *ViDoRe* w.r.t. different retrieval models. The  $mean \pm std$  size is given for the sparse embeddings. In general multiple vectors (2-5) per page are used for BGE-M3 and BM25.

### B.4 LATENCY COMPUTATIONS

To ensure comparison fairness, the latencies of the different retrieval systems shown in Figure 2 are measured on the same g2-standard-8 GCP VM with a NVIDIA L4 GPU. Document pages are embedded using the highest settings of Unstructured with captioning (see subsection 3.2). SigLIP

<sup>18</sup><https://pytorch.org/>

<sup>19</sup><https://huggingface.co>

<sup>20</sup>URL of community blogposts with experimental details of binarized ColPali vectors will be inserted after anonymity period

and *ColPali* are both loaded with `bf16` parameter dtypes. The reported times in Table 5 are the average per-page latencies for each indexing operation on 1000 randomly chosen documents across all splits of the *ViDoRe* benchmark test set. A batch size of 8 was used for the BGE-M3 model used with *Unstructured*, and a batch size of 4 was used for *SigLIP* and *ColPali*.

Indexing operation	Latency (s)		
	Unstructured	SigLIP	ColPali
Layout detection	0.81	NA	NA
OCR	2.67	NA	NA
Captioning	3.71	NA	NA
Page encoding	0.03	0.12	0.39
Total	7.22	0.12	0.39

Table 5: Page-level latencies for document indexing using various retrieval systems. *SigLIP* and *ColPali* are much faster than *Unstructured* because they don’t require the layout detection, OCR, and captioning operations.

## B.5 CAPTIONING

Examples of captions generated for visually rich document chunks with Claude-3 Sonnet are shown in Figure 5 and Figure 4. The prompt used for generating the description is the following:

You are an assistant specialized in document analysis. Given a table or a figure, you have to provide a detailed summary of the content in maximum 3000 characters. Your summary should be qualitative and not quantitative. Here is the table/figure to analyze: {image}. Answer ONLY with the caption of the table/figure.

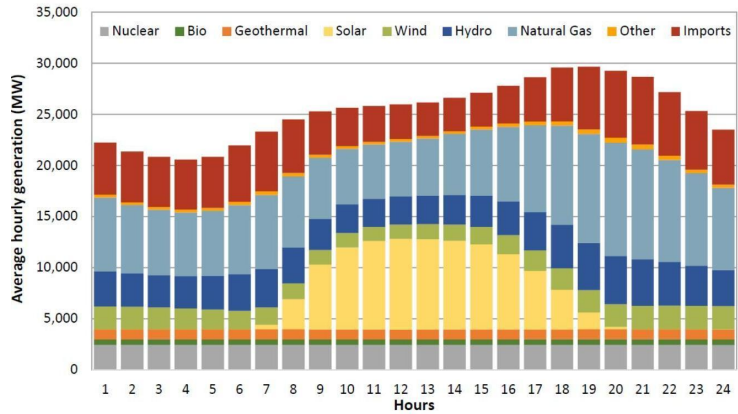


Figure 4: Example from the “Energy” test set.

**Caption:** The image depicts the hourly energy generation profile, illustrating the contributions of various energy sources over 24 hours. The data is presented as a stacked bar chart, with the x-axis representing the hours of the day from 1 to 24, and the y-axis showing the average hourly generation in MW. The bars are segmented into different colors, each representing a distinct energy source: nuclear, bio, geothermal, solar, wind, hydro, natural gas, and other imports. The chart provides insights into the temporal variations in energy generation across different sources, highlighting the interplay between baseload and intermittent sources throughout the day.

1026  
1027  
1028  
1029  
1030  
1031  
1032  
1033  
1034  
1035  
1036  
1037  
1038  
1039  
1040  
1041  
1042  
1043  
1044  
1045  
1046  
1047  
1048  
1049  
1050  
1051  
1052  
1053  
1054  
1055  
1056  
1057  
1058  
1059  
1060  
1061  
1062  
1063  
1064  
1065  
1066  
1067  
1068  
1069  
1070  
1071  
1072  
1073  
1074  
1075  
1076  
1077  
1078  
1079

Document	System of Record <sup>1</sup>						
	County Servers	Project View	OnBase	CGI Advantage Financial System	Purchasing Department		
Project plan/scope	W	T					
Project budgets	W	T	W	T			
Schedules/timeline (design)	W	T	W	T			
Schedules/timeline (construction)	W	T	W				
Executed contracts	T			W	T		
Purchase orders	T		W		W	T	
Solicitation advertisements	T		W	T	W	T	
Proposal submissions	T		W		W	T	
Selection committee evaluation documents	T		W	T	W	T	
Independent cost estimates	T	W	T	W	T	W	T
Negotiation details	T		W			W	
Notice of award	T		W			W	
Notice to proceed	T		W			W	
Invoices/applications for payment ("AFP")		W	T	W	W	T	
Change order requests	T		W				
Approved change orders	T	W	T	W			
Requests for Information (RFI)	W	T				W	T
Bid submissions			W			W	T
Shop drawings	W	T		T			
Photographs	W	T					
As-builts	W	T		T			
Operating manuals	W	T					
Maintenance schedules	W	T					
Warranties	W	T		T			
Daily diaries	N/A	T					
Weekly meeting minutes	W	T					
Monthly progress reports	W	T					
Allowance usage logs	W	T					
Punch lists	W	T					
Insurance records	T		W				

Figure 5: Example from the “Government Reports” test set.  
**Caption:** The image shows a table titled “System of Record” which outlines the different types of documents or records maintained across various systems or departments within an organization related to project management and construction. The rows list documents like project plans, budgets, schedules, contracts, purchase orders, invoices, change requests, bid submissions, drawings, manuals, meeting minutes, and reports. The columns indicate the system or department responsible for maintaining each record, such as County Servers, Project View, OnBase, CGI Advantage Financial System, and Purchasing Department. The table uses “W” and “T” markers to denote which system or department serves as the primary source (writer) or storage location (trailer) for each type of document.

## C ADDITIONAL RESULTS

### C.1 OTHER METRICS

	ArxivQ	DocQ	InfoQ	TabF	TATQ	Shift	AI	Energy	Gov.	Health.	Avg.
<b>Unstructured</b> <small>text-only</small>											
BM25	-	26.6	-	-	34.6	45.0	86.0	70.0	68.0	74.0	-
BGE-M3	-	22.8 <sub>↓3.8</sub>	-	-	26.1 <sub>↓8.5</sub>	51.0 <sub>↑6.0</sub>	81.0 <sub>↓5.0</sub>	72.0 <sub>↑2.0</sub>	67.0 <sub>↓1.0</sub>	77.0 <sub>↑3.0</sub>	-
<b>Unstructured</b> <small>+ ocr</small>											
BM25	26.7	28.9	54.0	30.4	50.0	52.0	86.0	77.0	74.0	80.0	55.9
BGE-M3	28.1 <sub>↑1.4</sub>	22.9 <sub>↓6.0</sub>	53.8 <sub>↓0.2</sub>	55.7 <sub>↑25.3</sub>	38.6 <sub>↓11.4</sub>	<b>56.0</b> <sub>↑4.0</sub>	82.0 <sub>↓4.0</sub>	79.0 <sub>↑2.0</sub>	76.0 <sub>↑2.0</sub>	83.0 <sub>↑3.0</sub>	57.5 <sub>↑1.6</sub>
<b>Unstructured</b> <small>+ Captioning</small>											
BM25	35.5	30.2	61.5	24.3	49.0	47.0	79.0	76.0	75.0	81.0	55.9
BGE-M3	29.3 <sub>↓6.2</sub>	26.0 <sub>↓4.2</sub>	62.1 <sub>↑0.6</sub>	58.6 <sub>↑34.3</sub>	30.6 <sub>↓18.4</sub>	55.0 <sub>↑8.0</sub>	80.0 <sub>↑1.0</sub>	78.0 <sub>↑2.0</sub>	69.0 <sub>↓6.0</sub>	83.0 <sub>↑2.0</sub>	57.2 <sub>↑1.3</sub>
<b>Contrastive VLMs</b>											
Jina-CLIP	19.4	7.3	26.7	12.5	1.6	2.0	11.0	13.0	15.0	17.0	12.6
Nomic-vision	10.4	6.7	22.1	9.6	1.6	0.0	9.0	9.0	7.0	13.0	8.8
SigLIP (Vanilla)	34.2	21.3	51.8	46.1	17.9	13.0	50.0	51.0	47.0	65.0	39.7
<b>Ours</b>											
(Copied) SigLIP (Vanilla)	34.2	21.3	51.8	46.1	17.9	13.0	50.0	51.0	47.0	65.0	39.7
BiSigLIP <small>(+fine-tuning)</small>	49.2 <sub>↑15.0</sub>	23.8 <sub>↑2.5</sub>	59.0 <sub>↑7.2</sub>	52.1 <sub>↑6.0</sub>	20.7 <sub>↑2.8</sub>	16.0 <sub>↑3.0</sub>	62.0 <sub>↑12.0</sub>	61.0 <sub>↑10.0</sub>	55.0 <sub>↑8.0</sub>	72.0 <sub>↑7.0</sub>	47.1 <sub>↑7.4</sub>
BiPali <small>(+LLM)</small>	46.4 <sub>↓2.8</sub>	20.0 <sub>↓3.8</sub>	54.6 <sub>↓4.4</sub>	63.2 <sub>↑11.1</sub>	20.4 <sub>↓0.4</sub>	34.0 <sub>↑18.0</sub>	59.0 <sub>↓3.0</sub>	45.0 <sub>↓16.0</sub>	57.0 <sub>↑2.0</sub>	56.0 <sub>↓16.0</sub>	45.6 <sub>↓1.5</sub>
ColPali <small>(+Late Inter.)</small>	<b>72.4</b> <sub>↑26.0</sub>	<b>45.6</b> <sub>↑25.6</sub>	<b>74.6</b> <sub>↑20.0</sub>	<b>75.4</b> <sub>↑12.1</sub>	<b>53.1</b> <sub>↑32.7</sub>	55.0 <sub>↑21.0</sub>	<b>93.0</b> <sub>↑34.0</sub>	<b>85.0</b> <sub>↑40.0</sub>	<b>85.0</b> <sub>↑28.0</sub>	<b>88.0</b> <sub>↑32.0</sub>	<b>72.7</b> <sub>↑27.1</sub>

Table 6: **Comprehensive evaluation of baseline models and our proposed method on ViDoRe.** Results are presented using Recall@1 metrics. Text-only metrics are not computed for benchmarks with only visual elements.

### C.2 MODEL VARIANTS

	ArxivQ	DocQ	InfoQ	TabF	TATQ	Shift	AI	Energy	Gov.	Health.	Avg.
ColSigLIP (PaliGemma)	3.1	3.0	5.1	6.2	2.5	1.0	3.4	3.4	2.3	2.2	3.2
BiSigLIP (PaliGemma)	18.5	14.6	33.4	39.5	16.1	5.2	27.6	32.6	36.6	35.7	26.0
ColSigLIP (Original)	2.6	2.2	2.3	5.7	1.8	1.0	2.6	4.1	1.4	1.5	2.5
ColPali (No Q.A. Tokens)	80.4	53.2	82.4	77.4	65.7	63.4	97.0	89.9	93.6	92.4	79.6
ColPali (Docmatix)	71.3	48.0	80.0	83.9	59.1	73.8	95.7	93.8	92.5	93.1	79.1
ColPali (224)	71.0	37.4	62.3	65.7	28.6	20.4	65.7	66.8	73.9	73.0	56.5
ColPali (Vision Trained)	78.8	53.9	81.3	81.7	64.4	70.6	95.3	91.7	93.5	94.7	80.6
ColPali (No Pairwise)	79.0	53.0	82.1	85.3	63.2	66.2	94.9	88.9	92.7	92.1	79.7
ColPali (+TabFQuAD training)	77.6	54.7	82.6	86.5	65.4	73.9	94.8	92.4	94.2	94.8	81.7
ColIdeFics2 (64)	73.6	48.0	82.4	81.6	63.0	57.2	95.5	86.9	86.6	91.2	76.6
ColQwen2 (768)	86.4	56.2	89.8	88.7	75.2	85.7	98.8	94.8	93.2	97.3	86.6
ColPali (Reference: 448)	79.1	54.4	81.8	83.9	65.8	73.2	96.2	91.0	92.7	94.4	81.3

Table 7: **Benchmark scores for the “negative results” and various ablations on ViDoRe; ColPali for reference.** Results are presented using nDCG@5 metrics. Text-only metrics are not computed for benchmarks with only visual elements.

1134  
1135  
1136  
1137  
1138  
1139  
1140  
1141  
1142  
1143  
1144  
1145  
1146  
1147  
1148  
1149  
1150  
1151  
1152  
1153  
1154  
1155  
1156  
1157  
1158  
1159  
1160  
1161  
1162  
1163  
1164  
1165  
1166  
1167  
1168  
1169  
1170  
1171  
1172  
1173  
1174  
1175  
1176  
1177  
1178  
1179  
1180  
1181  
1182  
1183  
1184  
1185  
1186  
1187



**Query:** "Quelle partie de la production pétrolière du Kazakhstan provient de champs en mer ?"

Figure 6: Similarity of the image patches w.r.t. the underlined token in the user query. This example is from the *Shift* test set.

## D MORE SIMILARITY MAPS

In Figure 3, *ColPali* assigns a high similarity to all patches with the word “Kazakhstan” when given the token `<_Kazakhstan>`. Moreover, our model seems to exhibit world knowledge capabilities as the patch around the word “Kashagan” - an offshore oil field in Kazakhstan - also shows a high similarity score.

It is also interesting to highlight that both this similarity map and the one displayed in Figure 3 (right) showcase a few white patches with high similarity scores. This behavior might first seem surprising as the white patches should not carry a meaningful signal from the original images. We believe the vectors associated with these patches share a similar role with the ViT registers (Darcet et al., 2023), i.e. these patches were repurposed for internal computations and stored the global information from the whole image.

## E MODEL GLOSSARY

### SigLIP

SigLIP (Sigmoid Loss for Language Image Pre-Training) builds upon CLIP (Contrastive Language-Image Pretraining)—a foundational model that aligns images and text by maximizing the similarity between correct image-text pairs while minimizing it for incorrect ones, leveraging a contrastive loss (Zhai et al., 2023). Unlike CLIP (Radford et al., 2021), which applies the softmax function to the logits, SigLIP uses the sigmoid activation function. This innovation eliminates the need for a global view of all pairwise similarities between images and texts within a batch, enabling more flexible batch size scaling (up to 1M items per batch, with an effective optimal batch size of 32k). This approach allows SigLIP to achieve state-of-the-art performance in zero-shot image classification tasks.

### PALIGEMMA

PaliGemma is a 3B-parameter vision-language model. It integrates the SigLIP vision encoder with a Gemma-2B language decoder, connected via a multimodal linear projection layer (Lucas Beyer\* et al.,

1188 2024). The model processes images by segmenting them into a fixed number of Vision Transformer  
1189 (Dosovitskiy et al., 2020) tokens, which are prepended to an optional text prompt.

1190 A distinguishing feature of PaliGemma is its operation as a Prefix-Language Model (Prefix-LM).  
1191 This design ensures full attention between image tokens and the user-provided input (prefix) while  
1192 generating outputs auto-regressively (suffix). This architecture allows image tokens to access the  
1193 task-specific query during processing, facilitating more effective task-dependent reasoning.

1194 PaliGemma was trained in four stages: unimodal pretraining with existing components, extended  
1195 multimodal pretraining, short high-resolution pretraining, and task-specific fine-tuning.

1197

## 1198 COLBERT

1199 ColBERT (Contextualized Late Interaction over BERT) is a retrieval model designed to balance speed  
1200 and effectiveness in information retrieval tasks (Khattab & Zaharia, 2020). Traditional retrieval models  
1201 are typically categorized based on their type of interaction: either processing queries and documents  
1202 independently for efficiency (bi-encoders) or jointly to capture rich contextual relationships (cross-  
1203 encoders). ColBERT combines the advantages of both approaches through a novel late interaction  
1204 mechanism.

1205 Queries and documents are encoded separately using BERT, enabling offline pre-computation of  
1206 document representations for scalability. Instead of pooling embeddings into a single vector, ColBERT  
1207 retains token-level embeddings and employs a MaxSim operator to compute fine-grained similarity  
1208 scores. For each query token, the model determines the maximum similarity with document tokens,  
1209 summing these scores to compute relevance.

1210 This architecture preserves the contextual richness of deep language models while significantly  
1211 improving computational efficiency. By delaying the interaction step, ColBERT supports vector  
1212 similarity indexing, facilitating end-to-end retrieval from large collections without prohibitive costs.  
1213 Empirical evaluations on passage search datasets demonstrate that ColBERT achieves competitive  
1214 effectiveness compared to existing BERT-based models (Devlin et al., 2018), while executing queries  
1215 orders of magnitude faster and with drastically reduced computational requirements.

1216

1217

1218

1219

1220

1221

1222

1223

1224

1225

1226

1227

1228

1229

1230

1231

1232

1233

1234

1235

1236

1237

1238

1239

1240

1241

# F EXAMPLES FROM THE ViDoRe BENCHMARK

1242  
1243  
1244  
1245  
1246  
1247  
1248  
1249  
1250  
1251  
1252  
1253  
1254  
1255  
1256  
1257  
1258  
1259  
1260  
1261  
1262  
1263  
1264  
1265  
1266  
1267  
1268  
1269  
1270  
1271  
1272  
1273  
1274  
1275  
1276  
1277  
1278  
1279  
1280  
1281  
1282  
1283  
1284  
1285  
1286  
1287  
1288  
1289  
1290  
1291  
1292  
1293  
1294  
1295

**Query:** What types of accounts or products allow investors to defer paying taxes?

**Tax-efficient investing**  
Taxes have the potential to significantly affect your investment returns.

**Takeaway:** Retirement savings accounts—including 401(k) and 403(b) plans, IRAs, health savings accounts (HSAs), and other tax-advantaged products—each have distinct advantages and allow you to defer paying taxes.

**Message:** Using great location strategies, investing in lower-cost funds, understanding mutual fund distributions, and taking advantage of hardship gifts and capital loss deductions can all help you manage your tax burden.

**Takeaway:** Consider tax-free investments, municipal bonds, HSAs, and college savings accounts to help reduce your taxes.

**Net Savings Over PV System Useful Life**

Scenario	Net Savings Over PV System Useful Life
100% Solar	\$1,048
80% Solar	\$931
50% Solar	\$518
20% Solar	\$131

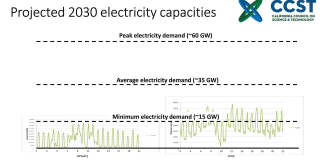
**Query:** What is the estimated to-Query: What is the projected total savings for a PV system in peak electricity demand in California under the net metering fornia for the year 2030? (flat rate) billing option over the system's useful life of 25 years?

**Net Savings Over PV System Useful Life**

Rate/Billing Option	City	Low System Cost	Flat Rate System Cost	High System Cost
Net Metering (Flat Rate)	Charlotte	\$1,048	\$931	\$518
	Charlotte	\$900	\$783	\$475
Time-of-Day Billing	Charlotte	\$668	\$551	\$338
	Charlotte	\$551	\$434	\$221
Flat Rate	Charlotte	\$1,100	\$983	\$570
	Charlotte	\$900	\$783	\$475
NC GreenPower Option 1	Charlotte	\$800	\$683	\$270
	Charlotte	\$712	\$595	\$182

**Table 3. Net Savings Over PV System Useful Life**

NC GreenPower has the advantage of paying customers a premium for their RECs for the first five years, which can also help pay back the costs of the system and reduce interest payments. However, it does not provide as much savings over the life of the system as the other options, since the NC GreenPower credit is limited to 5 years, and the amount each



## Artificial Intelligence

**Query:** What are some common outcome areas targeted by TAI for different age groups?

**Technology Aided Instruction and Intervention (TAII)**

**Outcome Areas**

Age Group	Communication	Social	Academic	Physical	Mental Health	Self-Determination
0-5	✓	✓	✓	✓	✓	✓
6-12	✓	✓	✓	✓	✓	✓
13-18	✓	✓	✓	✓	✓	✓
19-25	✓	✓	✓	✓	✓	✓
26-35	✓	✓	✓	✓	✓	✓
36-45	✓	✓	✓	✓	✓	✓
46-55	✓	✓	✓	✓	✓	✓
56-65	✓	✓	✓	✓	✓	✓
66-75	✓	✓	✓	✓	✓	✓
76-85	✓	✓	✓	✓	✓	✓
86-95	✓	✓	✓	✓	✓	✓

**Query:** What did the robot monitor to determine when to activate or deactivate the blower motor and blinker?

**Robot Monitoring System**

The robot monitors the following parameters to determine when to activate or deactivate the blower motor and blinker:

- Temperature
- Humidity
- Light intensity
- Sound level
- Proximity to obstacles
- Position relative to the field

When any of these parameters reach a predefined threshold, the robot triggers the corresponding action (e.g., turning on the blower motor or activating the blinker).

**Query:** What is the key approach used in the PDP architecture?

**PDP Machine Architecture**

The key approach used in the PDP architecture is the use of an adaptive filter. The adaptive filter can accept a real-world analog input and compare it to a stored pattern. The stored pattern represents the desired input level which can then be modified as necessary by the echo-free signals can be produced the correct results. A more abstract approach driving the design of the PDP network is machine efficiency, that is, the optimal utilization of the total computer capacity. In the more familiar structure of a modern computer (the von Neumann architecture) parts of the computer's capacity is its memory. It can be used for most of the time. This is very wasteful from a pure resource management standpoint. The PDP machine addresses the problem by using many processors and memories, but does so

**Learning rule:**

$$W_{ij} = w_{ij} + \frac{1}{N} \sum_{k=1}^N (Output_k - Threshold_k) \cdot Input_{ij}^k$$

**Figure 1. Schematic diagram of a PDP Network**



1296  
1297  
1298  
1299  
1300  
1301  
1302  
1303  
1304  
1305  
1306  
1307  
1308  
1309  
1310  
1311  
1312  
1313  
1314  
1315  
1316  
1317  
1318  
1319  
1320  
1321  
1322  
1323  
1324  
1325  
1326  
1327  
1328  
1329  
1330  
1331  
1332  
1333  
1334  
1335  
1336  
1337  
1338  
1339  
1340  
1341  
1342  
1343  
1344  
1345  
1346  
1347  
1348  
1349

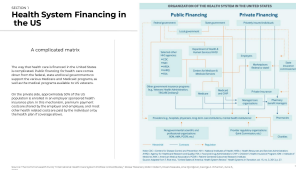
## Healthcare Industry

**Query:** What is the chemical formula for the ferroelectric material Lead Zirconium Titanate (PZT)?

**Ferroelectrics** UCLA

- Lead Zirconium Titanate
  - PZT
  - $Pb(Zr_{1-x}Ti_x)_2O_7$
  - 1952 Shirane, Suzuki :  $Pb(Zr_{1-x}Ti_x)_2O_7$  solid solutions
  - 1955 Jaffe, Cook, Berlincourt, Gerson: Complete study of PZT formulations
  - Curie temperature 170-360

**Query:** What government entities are involved in public financing for healthcare in the US?



**Query:** What does the AVPU scale stand for in assessing the level of consciousness of a seriously ill child?

**Assessment of the seriously ill child**

**AVPU Scale:** Alert, Verbal, Pain, Unresponsive.

**Capillary refill time:** A simple test to check for perfusion. Normal is less than 2 seconds.

**Advanced life support (ALS):** Includes airway management, oxygenation, ventilation, and circulatory support.

**Basic life support (BLS):** Includes airway management, oxygenation, ventilation, and circulatory support.

**The seriously injured child:** Management of the seriously injured child must take account of potential injury to the cervical spine and other bones and internal organs (Fig. 4.7).

## Government Reports

**Query:** What are some mandates for the EPA under the Pollution Prevention Act?

**APPENDIX II – CURRENT POLLUTION PREVENTION MANDATES IN FEDERAL STATUTES**

Federal Act	Section	Pollution Prevention Mandate
National Pollution Discharge Elimination Act (NPDES)	13104	EPA is authorized to develop and implement a strategy to promote source reduction.
	13105	EPA is authorized to develop and implement a strategy to provide grants to the States to promote source reduction for businesses.
Clean Air Act (CAA)	7402	Owners and operators of businesses that are required to file a toxic chemical release form must include a toxic reduction and recycling report.
	7403	EPA is authorized to establish a national research and development program for prevention and air pollution control.
	7405	Also, EPA must facilitate coordination among air pollution prevention and control agencies.
	7412	EPA can make grants to air pollution prevention and control agencies.
	7413	Facilities that reduce their emission of ozone are eligible for 90% tax credit for permit payments.
	7414 and 7418	EPA may establish research, monitoring, and modeling for air facilities that emit pollutants.
Subchapter I, Part C, Sec. 2475-2479		Prevention of significant deterioration of air quality establishment of a plan that includes emission limitations to prevent public welfare and the environment.
	Subchapter II	General emissions standards

**Query:** What is the strategy of KPMG Hazem Hassan?

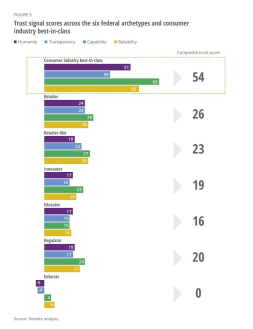
**Who we are?**

**Our mission:** KPMG Hazem Hassan is a professional services firm that delivers high-quality and advisory services to our clients and employees in the Middle East, North Africa, and Europe.

**Our strategy:** Our strategy is to be the most trusted and most innovative advisory firm in the Middle East, North Africa, and Europe.

**Our values:** Integrity, Innovation, and Client Focus.

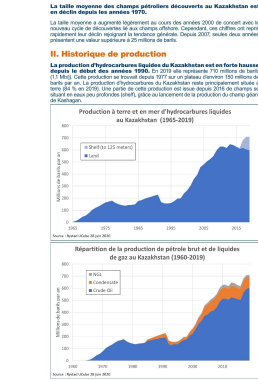
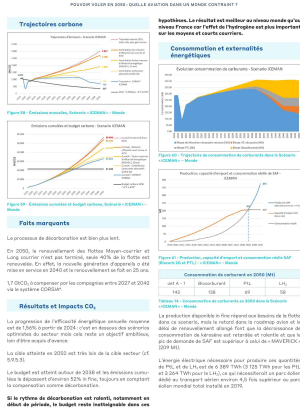
**Query:** What is the trust signal score for the consumer industry best-in-class archetype?



1350  
1351  
1352  
1353  
1354  
1355  
1356  
1357  
1358  
1359  
1360  
1361  
1362  
1363  
1364  
1365  
1366  
1367  
1368  
1369  
1370  
1371  
1372  
1373  
1374  
1375  
1376  
1377  
1378  
1379  
1380  
1381  
1382  
1383  
1384  
1385  
1386  
1387  
1388  
1389  
1390  
1391  
1392  
1393  
1394  
1395  
1396  
1397  
1398  
1399  
1400  
1401  
1402  
1403

### Shift

**Query:** Selon le graphique, quelle est la capacité d'import et la consommation réelle de carburants SAF (biocarburants durables pour l'aviation) prévues en 2050 ?



**Query:** Quels sont les pays ayant la plus grande part des découvertes cumulées de pétrole brut en 2020 (en milliers de barils, hors découvertes cumulées) ?

